

Synthesis and characterization of perylene–bithiophene–triphenylamine triads: studies on the effect of alkyl-substitution in p-type NiO based photocathodes†

Martin Weidelener,^a Amaresh Mishra,^{*a} Andrew Nattestad,^{bd} Satvasheel Powar,^c Attila J. Mozer,^d Elena Mena-Osteritz,^a Yi-Bing Cheng,^b Udo Bach^{*b} and Peter Bäuerle^{*a}

Received 26th December 2011, Accepted 6th February 2012

DOI: 10.1039/c2jm16847b

We report the synthesis of new donor– π –acceptor (D– π –A) dyes and their application in dye-sensitized solar cells (DSCs) with nickel(II) oxide (NiO)-based photocathodes. These D– π –A sensitizers incorporate a triphenylamine donor, a bithiophene π -bridge, and a perylenemonoimide (PMI) acceptor group. Two carboxylate groups attached to the triphenylamine afford strong anchoring to the NiO surface. The dyes in this series were varied firstly by the inclusion of an ethynyl linker between bithiophene and the triphenylamine moieties (**1** vs. **2**), thereby increasing the length of the conjugated bridge. Despite very similar optoelectronic properties, the ethynyl-containing dye **2** showed a $\sim 25\%$ improvement in power conversion efficiency in p-DSCs compared to **1**, mostly attributed to the increased current density. Contrary to initial expectations, there was no major influence of the distance between the PMI unit of the dye and the NiO surface on the photoinduced dye anion lifetime, as measured by nanosecond transient absorption spectroscopy (TAS). Furthermore, altering the position of the alkyl chains on the bridging bithiophene in **3** and **4** resulted in a modest red shift in the dye absorption on account of increased charge delocalisation between the PMI and the π -bridge, owing to a reduced torsion angle between the PMI and the adjacent thiophene unit. Quantum-chemical DFT calculations were performed in order to evaluate these torsion angles and to study their influence on the electron density distribution in the relevant molecular orbitals. These changes of the molecular structure of the isomeric dyes **3** and **4** did not translate into improved photovoltaic performance, which is primarily attributed to lower charge photogeneration rates probed by transient absorption spectroscopy. While for p-type DSCs impressive overall solar-to-electric conversion efficiency of 0.04–0.10% under full sun illumination (simulated AM1.5G sunlight, 100 mW cm⁻²) and a broad incident photon to current efficiency (IPCE) response (350–700 nm) is demonstrated for these new dyes, the study clearly shows the need for judicious design rules for p-type sensitizers for application in photocathodic DSCs.

Introduction

The direct conversion of solar energy to electricity is expected to provide a significant contribution to the renewable energy sector

in coming years. In this context, n-type dye-sensitized solar cells (n-DSCs) have attracted considerable attention with state-of-the-art DSCs displaying overall power conversion efficiencies (η) in excess of 12%.^{1–5} These devices utilise Ru(II)-polypyridyl complexes or metal-free organic dyes as the photoactive material which are adsorbed onto a high surface area mesoporous n-type titanium dioxide (TiO₂) along with a catalytic cathode typically from platinum.^{6,7} In this case, photocurrent results from electron injection from a photoexcited dye into the n-type semiconductor. In contrast, dye-sensitized photocathodic solar cells (p-DSCs) operate in an inverse mode with the transfer of a hole from a photoexcited dye to the valence band of a p-type semiconductor such as NiO. Although some organic dyes such as erythrosin B,⁸ coumarin^{9–12} and perylene derivatives¹³ have been used as sensitizers for p-DSCs, recent studies have shown that for

^aInstitute for Organic Chemistry II and Advanced Materials, University of Ulm, Albert-Einstein-Allee 11, 89081 Ulm, Germany. E-mail: amaresh.mishra@uni-ulm.de; peter.baeuerle@uni-ulm.de

^bARC Centre of Excellence for Electromaterials Science, Department of Materials Engineering, Monash University, Clayton, Victoria, Australia. E-mail: udo.bach@monash.edu

^cARC Centre of Excellence for Electromaterials Science, School of Chemistry, Monash University, Clayton, Victoria, 3800 Australia

^dARC Centre of Excellence for Electromaterials Science, Intelligent Polymer Research Institute, AIIM Facility, Innovation Campus, University of Wollongong, New South Wales, 2522, Australia

† Electronic supplementary information (ESI) available. See DOI: 10.1039/c2jm16847b

efficient p-type NiO-based photocathodic sensitizers it is important that the anchoring groups are attached to the electron donor part of the dye molecule and that the acceptor unit should be spatially removed from the semiconductor surface.^{6,13–15}

Due to good chemical and photostability, as well as reasonable transparency, NiO represents to date the most successful p-type semiconductor used for construction of dye-sensitized photocathodes and of tandem np-DSCs, in which both electrodes are photoactive,^{8,12,13} although other metal oxide semiconductors have also been used.^{16,17} Photocurrent matching is an essential prerequisite for the realization of highly efficient tandem np-DSCs. Recently, we demonstrated a judicious design of D- π -A dyes which led to record efficiencies in p-DSCs and tandem np-DSCs.¹⁸ p-DSCs with peak incident photon to current efficiency (IPCE) values as high as 62% and overall efficiencies of up to 0.41% were observed using the perylenemonoimide-oligothiophene-triphenylamine (PMI-nT-TPA) triads. In tandem np-DSC devices record efficiencies of up to 2.42% were demonstrated. While these efficiencies constitute the best reported for p-type DSCs to date, photocurrent matching of efficient np-DSCs requires p-type sensitizers demonstrating high quantum efficiency over a spectral range complementary to their n-type counterparts. Due to intensive research efforts over the last two decades, the number of available efficient n-type sensitizers is very broad.⁶ Furthermore, there is a fairly well understood set of criteria governing charge injection, charge recombination and charge regeneration reactions in n-type DSCs.^{6,19} In contrast, p-type DSCs are still in their infancy with only a few reports highlighting the correlations between the molecular structure and their solar cell performance.^{13,18,20–23}

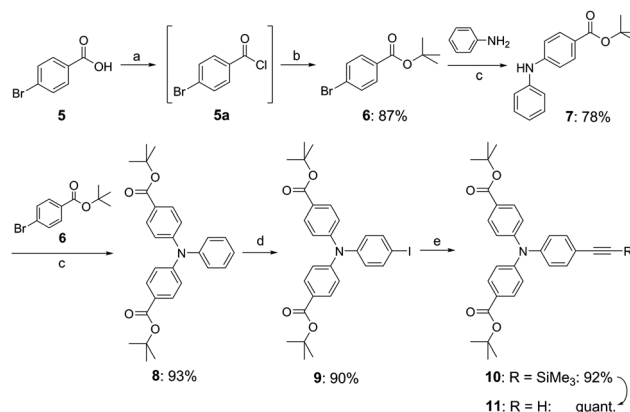
Herein, we present a further structural fine tuning of D- π -A dye **1** as a model for the series of PMI-nT-TPA. In derivative **2** an additional ethynylene unit is incorporated between the bridging bithiophene unit and the triphenylamine donor. D- π -A dyes **3** and **4** represent regioisomers to **1** and **2**, respectively, and bear the hexyl side chain at the other β -position in each thiophene ring of the bithiophene bridge. Instead of creating a distortion of the PMI and the adjacent 3-hexylthiophene unit in dyes **1** and **2**, in isomers **3** and **4** the steric repulsion is released (Chart 1). This was further confirmed by quantum-chemical DFT calculations. By shifting the alkyl chain position, the torsion angle between the perylene and thiophene units in **3** decreases, resulting in a more planar dye with red-shifted absorption. Changing the position of the alkyl chain (going from

dye **1** to **3**), however, results in steric hindrance between the triphenylamine and the bithiophene bridge, which was further reduced by the inclusion of an ethynyl unit in dye **4**. This series of dyes facilitates investigation into the effect of steric hindrances within sensitizing molecules for p-DSCs. The insertion of a rigid triple bond in dyes **2** and **4** increases the distance between the acceptor and the NiO surface. It was anticipated that this extra distance may affect the recombination kinetics between the photoinjected holes on NiO and electrons primarily located on the perylene unit of the photoreduced dye.

Results and discussions

Synthesis

Synthesis of triphenylamine building block **11** was achieved according to Scheme 1. 4-Bromo benzoic acid **5** was suspended in thionyl chloride and then stirred under reflux for 1 hour. After removal of the excess of thionyl chloride the intermediate 4-bromo benzoic acid chloride **5a** was reacted with potassium *tert*-butylate dissolved in THF at 0 °C to afford 4-bromo benzoic acid *tert*-butyl ester **6** in an overall 87% yield after bulb-to-bulb distillation.²⁴ Reaction of 1.5 eq. of aniline with 4-bromo benzoic acid *tert*-butyl ester **6** in a Pd⁰-catalyzed amination by using



Scheme 1 Synthesis of triphenylamine building block **11**. *Reagents and conditions:* (a) SOCl₂, reflux; (b) KO^tBu, THF, 0 °C; (c) Pd₂dba₃, [HP(*t*Bu)₃]BF₄, KO^tBu, toluene, rt; (d) ICl, Zn(OAc)₂, dioxane, rt; (e) trimethylsilylacetylene, CuI, Pd(PPh₃)₂Cl₂, piperidine, 60 °C; and (f) CsF, THF, methanol, rt.

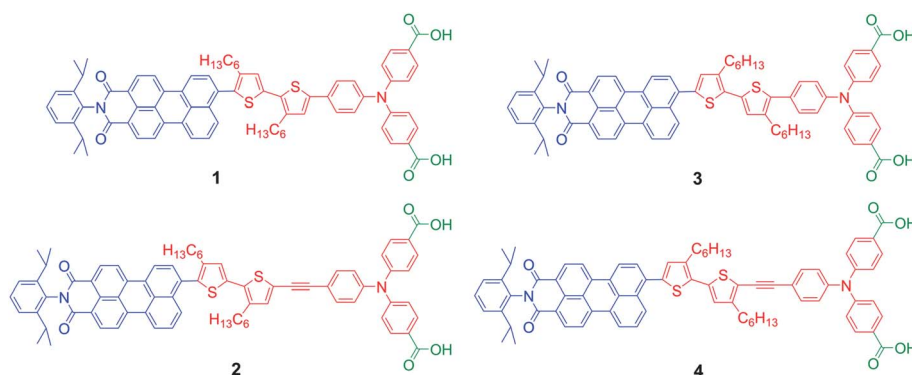
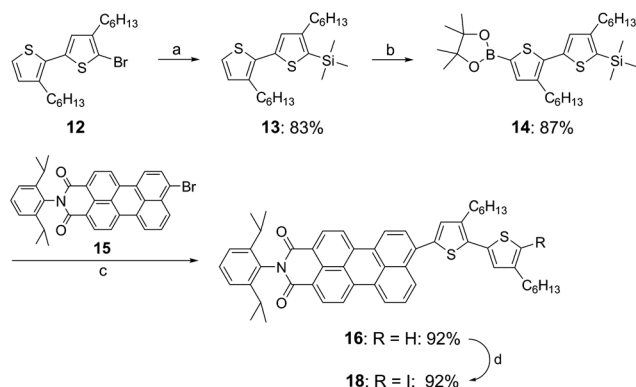


Chart 1 Structures of D- π -A dyes **1–4**.

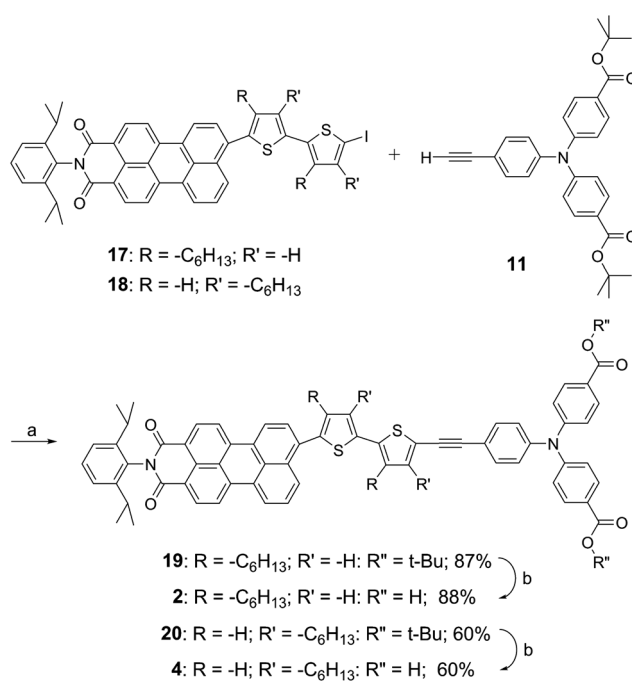
2.25 eq. of potassium *tert*-butylate in toluene at room temperature yielded 78% of diphenylamine **7** after recrystallization. Under similar conditions, diphenylamine **7** was reacted with 1.2 eq. of aryl bromide **6** to give corresponding triphenylamine **8** in 93% yield after column chromatography. Triphenylamine **8** was iodinated in dioxane using 2 eq. of iodine monochloride which had been activated by zinc acetate as Lewis acid.²⁵ Iodinated triphenylamine **9** was obtained in 90% yield after recrystallization. Ethynyl-triphenylamine building block **10** was synthesized by Pd⁰-catalyzed Sonogashira reaction of iodinated triphenylamine **9** and 1.5 eq. of trimethylsilylacetylene in piperidine. The reaction mixture was stirred at 60 °C for 3 hours and triarylamine **10** was obtained in 92% yield after chromatographic work-up. Deprotection of **10** using 3 eq. of caesium fluoride in a THF/methanol mixture afforded acetylene **11** in quantitative yield.

5-Bromo-3',4'-dihexyl-2,2'-bithiophene²⁶ **12** was lithiated with *n*-butyllithium (*n*-BuLi) in THF at -78 °C and successively quenched with trimethylsilyl (TMS) chloride to afford TMS-protected bithiophene **13** in 83% yield (Scheme 2). Lithiation of bithiophene **13** with *n*-BuLi in THF at -78 °C and subsequent addition of pinacol isopropyl borate led to boronic ester **14** in 87% yield (GC-purity: 90%), which was used for the next step without further purification. Perylenyl-bithiophene dyad **16** was synthesized by Pd⁰-catalyzed Suzuki-type cross-coupling reaction of brominated perylenemonoimide **15** and boronic ester **14** in THF at 60 °C and successive *in situ* deprotection of the TMS group using tetrabutylammonium fluoride. After column chromatography perylenyl-bithiophene **16** was obtained in an overall yield of 92%. Dyad **16** was iodinated using an effective mercury-mediated iodination procedure²⁶ to afford iodinated perylenyl-bithiophene **18** in 92% yield after column chromatography.

Regioisomeric perylenyl-bithiophene building blocks **17** (ref. 26) and **18** were reacted with freshly deprotected triphenylamine **11** in a Pd⁰-catalyzed Sonogashira reaction to afford corresponding triads **19** and **20** in 60 and 87% yield, respectively, after column chromatography (Scheme 3). The hydrolysis of the ester group in the case of **2** and **4** under acidic conditions using trifluoroacetic acid (TFA) was not successful. Therefore, the ester groups were saponified with lithium hydroxide in methanol



Scheme 2 Synthesis of perylenylbithiophene building block **18**. *Reagents and conditions:* (a) (1) *n*-BuLi, THF, -78 °C, (2) Me₃SiCl; (b) (1) *n*-BuLi, THF, -78 °C, and (2) pinacol isopropyl borate; (c) (1) Pd(PPh₃)₄, K₃PO₄, DME, 80 °C and (2) Bu₄NF; and (d) (1) Hg(OCp)₂, dichloromethane, rt and (2) I₂.



Scheme 3 Synthesis of perylenyl-oligothiophene-triphenylamines **2** and **4**. *Reagents and conditions:* (a) for **19**: CuI, Pd₂dba₃, [HP(*t*Bu)₃]BF₄, piperidine, rt; for **20**: CuI, Pd(PPh₃)₂Cl₂, diisopropylamine, toluene, rt and (b) LiOH, MeOH, THF, 70 °C.

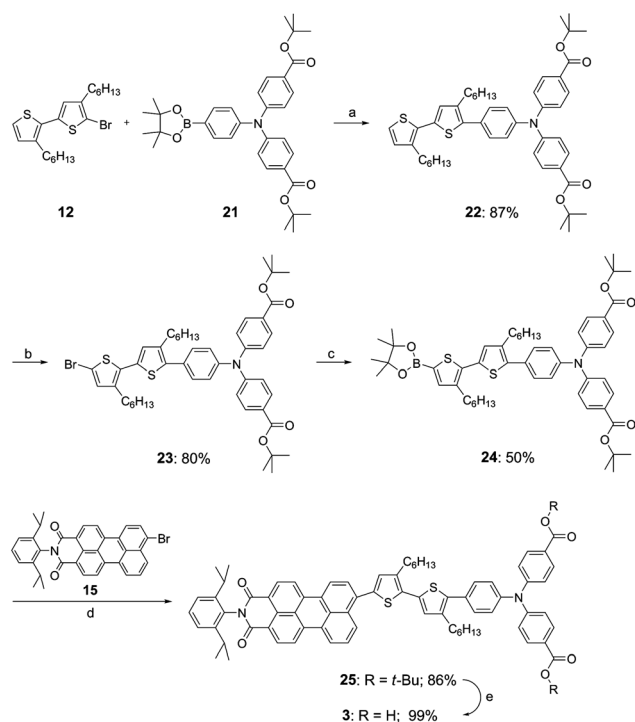
at 70 °C to give free acids **2** and **4** in 60 and 88% yields, respectively, after acidification with hydrochloric acid and filtration over a short column.

PMI-2T-TPA triad **3**, which is regioisomeric to parent dye **1**, was built up from bithiophene-triphenylamine dyad **22**, which was obtained by Pd⁰-catalyzed Suzuki-type coupling reaction of bromobithiophene **12** and triphenylamine boronic ester **21** in 87% yield after chromatographic work-up. Bromination of **22** at the free α -position of the terminal thiophene unit was carried out with *N*-bromosuccinimide (NBS) in DMF at -10 °C (Scheme 4). After column chromatography brominated dyad **23** was obtained in 80% yield.

Borylation of dyad **23** was obtained in a yield of about 50% (confirmed by ¹H-NMR) *via* magnesium-bromine exchange using isopropylmagnesium chloride and lithium chloride in THF at -10 °C and subsequent quenching with pinacol isopropyl borate. It was used for the next step without further purification. Pd⁰-catalyzed Suzuki-type reaction of bromoperyleneimide **15** and boronic ester **24** afforded PMI-2T-TPA triad **25** in 86% yield after chromatographic work-up. Triad **25** was hydrolyzed using TFA in dichloromethane at room temperature to give free acid **3** in quantitative yield after precipitation from *n*-hexane.

Optical properties

The UV-Vis absorption spectra of PMI-2T-TPA triads **1-4** showed an intense absorption band positioned at 520 to 530 nm (Table 1 and Fig. 1). The elongation of the donor part by a triple bond in **2** and **4** did not change the maximum of the low energy absorption band compared to triads **1** and **3**.^{27,28} However, the high energy absorption band, which corresponds to the donor



Scheme 4 Synthesis of perylenyl-oligothiophene-triphenylamine **3**. *Reagents and conditions:* (a) Pd(OAc)₂, PPh₃, K₃PO₄, THF, reflux; (b) NBS, DMF, -10 °C; (c) (1) isopropylmagnesium chloride, LiCl, THF, -10 °C and (2) pinacol isopropyl borate; (d) Pd(PPh₃)₄, K₃PO₄, THF, reflux; and (e) TFA, dichloromethane, rt.

unit ($\lambda_{\text{abs}} = \sim 360$ nm), is slightly broadened towards the lower energy region.

In comparison to the triads **1** and **2** the change of the hexyl positions in dyes **3** and **4** led to a red shift of about 10 nm and a broadening of the low energy absorption band. This might be due to a partial decoupling between the perylene and bithiophene π -orbitals, caused by a stronger twist between the perylene and bithiophene units in **1** and **2**, as a result of the hexyl chain close to the perylene unit. This assumption was supported by the observed low energy absorption band showing only one red-shifted maximum ($\lambda_{\text{max}} = \sim 528$ nm) for **3** and **4**, while one maximum and an additional shoulder ($\lambda_{\text{max}} = 518$ nm, $\lambda_{\text{max, sh}} = 498$ nm) in the case of **1** and **2**.

Fig. 1b shows the optical absorption of dyes **1–4** adsorbed onto the surface of transparent 0.9 μm thick NiO films with the absorption of the blank NiO film subtracted. Compared to solution spectra, dyes anchored at the NiO surface show blue-shifts of ~ 10 to 20 nm for the low energy absorption band, along with a spectral broadening. As a result of this broadening the onset of absorption onto the NiO film is extended to wavelengths of 650–670 nm. A spectral broadening is also commonly observed in the absorption of organic dyes adsorbed onto the surface of n-type TiO₂, which is ascribed to the electronic interactions of the dye with the semiconductor and adjacent dye molecules.^{29,30} The red shift in the low energy absorption band between the dyes in solution and attached to NiO is nearly identical for all dyes. The red shift associated with change in the hexyl chain position in regioisomer dyes **3** and **4** is also clearly observed on NiO making these dyes better light absorbers for p-type DSCs. The similar spectral shifts for each dye, as compared to solution, suggest there is no major difference in the orientation or packing of dye molecules on the NiO surface.

Electrochemical properties

Oxidation and reduction potentials of triads **1–4** were measured by cyclic voltammetry in dichloromethane and tetrabutylammonium hexafluorophosphate (*n*-Bu₄NPF₆) as a supporting electrolyte (Fig. 2). Redox potentials as well as electrochemically determined band gaps (ΔE_{CV}) are summarized in Table 1. In the oxidative regime, one oxidation process can be attributed to the perylene unit ($E^{\circ}_{\text{ox}3}$) while the remaining ones originate from the oxidation of the combined bithiophene and triarylamine donor. It is interesting to note that the first and second oxidation potentials ($E^{\circ}_{\text{ox}1}$ and $E^{\circ}_{\text{ox}2}$) of the ethynyl-containing dyes **2** and **4** are positively shifted compared to non-ethynylated counterparts **1** and **3**. This can be ascribed to the presence of the electron-withdrawing ethynylene group at the molecular backbone or by a conformational change of the thiophene and triphenylamine unit along the triple bond.^{28,31} The perylene oxidation of **2** ($E^{\circ}_{\text{ox}} = 1.10$ V) and **4** ($E^{\circ}_{\text{ox}} = 1.04$) is favoured over that of **1** ($E^{\circ}_{\text{ox}} = 1.15$ V) and **3** ($E^{\circ}_{\text{ox}} = 1.12$). The results demonstrated that the dications of ethynyl-containing dyes **2** and **4**, which are formed prior to the perylene oxidation, withdraw less electron density from the adjacent perylene than the donor dications of ethynyl-free dyes **1** and **3**. On the other hand, all triads showed

Table 1 Optical and electrochemical properties of the perylenyl-bithiophene-triphenylamine triads **1–4** in dichloromethane

	$\lambda_{\text{abs sol.}}^a$ /nm	$\epsilon/\text{L mol}^{-1} \text{cm}^{-1}$	$\lambda_{\text{abs film}}$ /nm	$E^{\circ}_{\text{ox}1}/\text{V}$	$E^{\circ}_{\text{ox}2}/\text{V}$	$E^{\circ}_{\text{ox}3}/\text{V}$	$E^{\circ}_{\text{red}1}/\text{V}$	$E^{\circ}_{\text{red}2}/\text{V}$	$E_{\text{HOMO}}^d/\text{eV}$	$E_{\text{LUMO}}^d/\text{eV}$	$\Delta E_{\text{CV}}^e/\text{eV}$
1	361 (57 200)		358, 502	0.51	0.69	1.15	-1.41	-1.88	-5.54	-3.80	1.74
	498 (41 600) ^b										
	518 (45 000)										
2	362 (61 800)		358, 502	0.62	0.75	1.10	-1.42	-1.87	-5.64	-3.84	1.80
	498 (39 200) ^b										
	519 (41 500)										
3	358 (53 800)		353, 521	0.48	0.67	1.12	-1.42	-1.86	-5.57	-3.76	1.81
	528 (43 100)										
4	362 (59 700)		358, 521	0.60	0.77	1.04	-1.37	-1.76	-5.47	-3.82	1.65
	530 (46 000)										

^a $c = 5 \times 10^{-5}$ mol L⁻¹. ^b Shoulder. ^c In dichloromethane/*n*Bu₄NPF₆ (0.1 M) vs. Fc/Fc⁺ at 100 mV s⁻¹. ^d Taken from the onset and related to the Fc/Fc⁺-couple with a calculated absolute energy of -5.1 eV. ^e Band gap calculated to $\Delta E = E_{\text{LUMO}} - E_{\text{HOMO}}$.

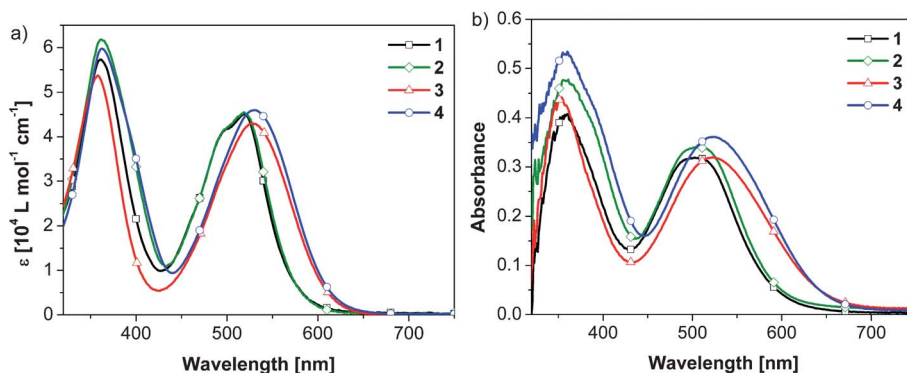


Fig. 1 (a) UV-Vis spectra of **1–4** in dichloromethane. (b) Absorption spectra of the sensitizers on a NiO film (NiO absorption subtracted).

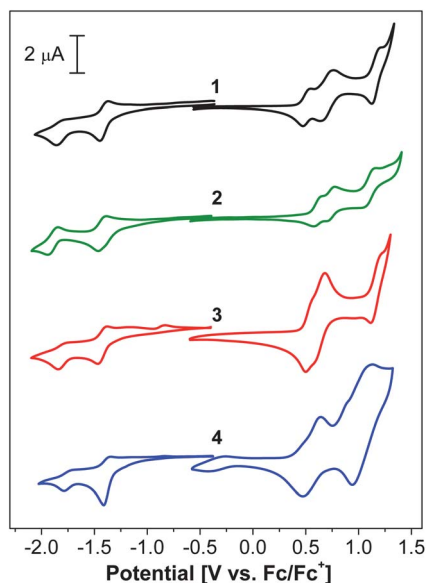


Fig. 2 Cyclic voltammograms of perylenyl-bithiophene–triphenylamines **1–4** in dichloromethane/*n*Bu₄NPF₆ (0.1 M) vs. Fc/Fc⁺ at 100 mV s⁻¹.

nearly identical electrochemical behaviour in the reductive regime, which corresponds to the two step reduction of the perylene unit at around -1.41 V and -1.87 V, respectively.

The HOMO levels of the triads calculated from electrochemical measurements were sufficiently lower than the valance band edge of NiO (~ -5.0 eV vs. vacuum or 0.5 V vs. NHE) enabling sufficient driving force for hole injection from the dye to the p-type semiconductor in DSCs. Equally, the LUMO energies of **1–4** are sufficiently above the redox potential of the iodide–triiodide redox couple, which should facilitate dye regeneration (Fig. 3).

Density functional theory (DFT) calculations with a B3LYP hybrid base (6-31G⁺(d,p)) were performed in order to evaluate the distortion between the perylene and the adjacent hexylthiophene unit and to analyse the electron distribution of the frontier orbitals. The HOMO–LUMO distribution of all dyes is shown in Fig. 4. The HOMO orbital distribution in dyes **3** and **4** is slightly more localized on the thiophene and TPA units, whereas in dyes **1** and **2** a more pronounced distribution on the PMI compared to the TPA part is observed. The differences in

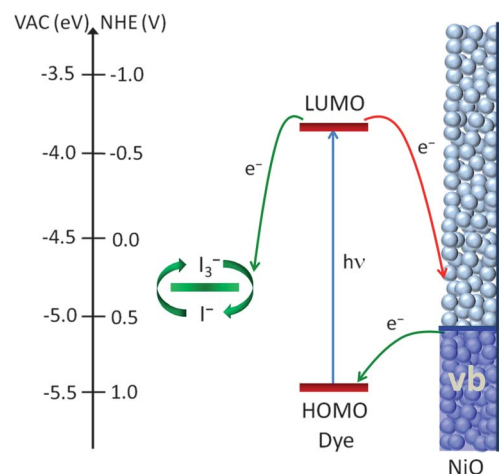


Fig. 3 Schematic representation of energy level diagram for electron transfer processes in p-type DSCs. The charge regeneration process is shown with green arrows and the charge recombination process with a red arrow.

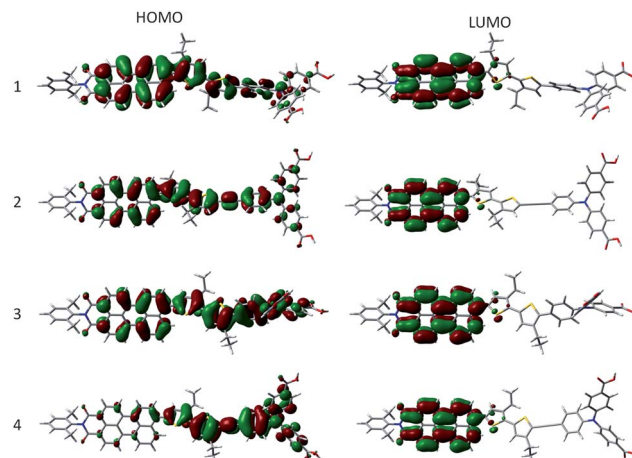


Fig. 4 Frontier orbitals distribution of dyes **1–4** calculated using the B3LYP (6-31G⁺(dp)) DFT method (carbons in *gray*, nitrogens in *blue*, oxygens in *red*, sulfurs in *yellow* and hydrogens in *white*). In order to accelerate the convergence of optimizations the long hexyl chains were replaced with ethyl substituents.

the HOMO orbital distribution are most probably due to a larger twist in the thiophene–PMI bond in dyes **1** and **2** that arises from the presence of the alkyl side chain close to the PMI unit (torsion angle $\sim 63^\circ$) compared to **3** and **4** (torsion angle = 54°). Consequently, a better electronic delocalization between PMI and thiophene parts can be expected in dyes **3** and **4** as manifested in the HOMO electronic distribution. In contrast, the LUMO orbital distribution is very similar for all dyes and localized almost entirely on the PMI unit.

The presence of the alkyl side chain on the TPA site in the case of dye **3** resulted in a large torsion angle of about 47.4° between the thiophene and phenyl units compared to dye **1** with a torsion angle of only 25° . The torsion between the TPA and adjacent thiophene unit was further reduced to planarity by the introduction of a triple bond (improper torsion angle = 0.9°) in dye **4**, while no significant difference was observed in the device performance as compared to dye **3** (*vide infra*).

Photovoltaic performance

For the potential application in DSCs the stability of the dyes is very important. This series of dyes are found to be highly stable under acidic and basic conditions. Current density–voltage (J – V) curves of devices based on dyes **1**–**4** are shown in Fig. 5 and the data are summarized in Table 2. The device measurements are very coherent and the data are reproducible within the given experimental accuracy. The results presented are repeated 3 times (different days) and are average over ~ 4 devices each.

The advantage of the presence of the ethynylene unit in triad **2** is reflected in an increased short circuit current density (J_{SC}) value by about 30% compared to parent dye **1**, roughly half the increase seen previously by going from a bithiophene to quaterthiophene bridge.¹⁸ Absorption data (Fig. 1), however, show little difference in the light-harvesting properties of dyes **1** and **2**. This improvement in J_{SC} is likely to arise from the retardation of charge recombination of the photoreduced dyes with holes in the NiO-photocathode. This assumption was made based on our previous observation that the tunnelling distance between

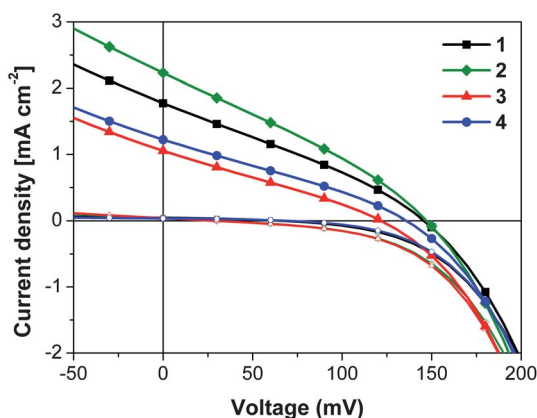


Fig. 5 Current–voltage (J – V) characteristics of devices under AM 1.5 simulated solar (100 mW cm^{-2}) illumination (filled symbols) and in the dark (open symbols) produced using $1.5 \mu\text{m}$ thick NiO electrodes, sensitized with dyes **1**–**4**. Electrolyte composition: 0.6 M *N*-methyl-*N*-butyl imidazoliumiodide, 0.5 M 4-*tert*-butylpyridine, 0.1 M guanidinium thiocyanate and 30 mM iodine in $85 : 15$ acetonitrile/valeronitrile.

Table 2 Photovoltaic parameters for devices made with $1.5 \mu\text{m}$ thick mesoporous NiO electrodes, sensitized with dyes **1**–**4** and sandwiched together with a platinized counter electrode at full sunlight (AM 1.5G, 100 mW cm^{-2})

	V_{OC}/mV	$J_{SC}/\text{mA cm}^{-2}$	Fill factor (%)	Efficiency (%)
1	146 ± 1	1.77 ± 0.04	30 ± 1	0.08 ± 0.01
2	147 ± 8	2.24 ± 0.01	30 ± 1	0.10 ± 0.01
3	122 ± 9	1.06 ± 0.09	29 ± 3	0.04 ± 0.01
4	136 ± 4	1.23 ± 0.22	28 ± 1	0.05 ± 0.01

electrons occupying the dye's LUMO and holes located in the semiconductor electrode strongly governs the observable recombination time constants.¹⁸ No change was observed in the open circuit voltage (V_{OC}) and FF values for dyes **1** and **2**. The device based on ethynyl-containing dye **2** showed the highest power conversion efficiency (PCE) of 0.10% among the dyes studied here, which is about 25% higher compared to dye **1**. In comparison to dye **1** device, a decrease in the V_{OC} and J_{SC} values was seen by changing the position of the hexyl chain in regioisomer dye **3**, thus, lowering the PCE to 0.04%. The introduction of a triple bond in regioisomer dye **4** slightly increases the J_{SC} value compared to dye **3**, and subsequently the overall PCEs for both dyes are very similar. The comparable performance of dyes **3** and **4** can be ascribed to the planarization of the perylene–thiophene units due to the different hexyl substitution pattern compared to **1** and **2**. The result further confirms that the partial decoupling between the acceptor and donor units appears to be essential for better device performance. Compared to dyes **1** and **3**, the J_{SC} values are increased for ethynyl-containing sensitizers, **2** and **4**, which could be ascribed to the improved injection and/or reduced recombination process.

IPCE responses of devices constructed using **1**–**4** are shown in Fig. 6 and correspond well with the measured J_{SC} values given in Table 2. Compounds **1** and **2** exhibit broad IPCE spectra ranging from 350 up to 650 nm region, which is extended to 700 nm for dyes **3** and **4**. The IPCE spectrum of dye **1** showed a maximum of about 16% at both absorption peaks of 380 and 503 nm. An increase in the IPCE peak maximum to 22% was observed by the insertion of an ethynylene group in dye **2**. The result is also consistent with their absorption spectra in thin films, thus, showing the contribution of absorption bands to the IPCE and J_{SC} . In contrast, the regioisomeric dye **3** showed an IPCE

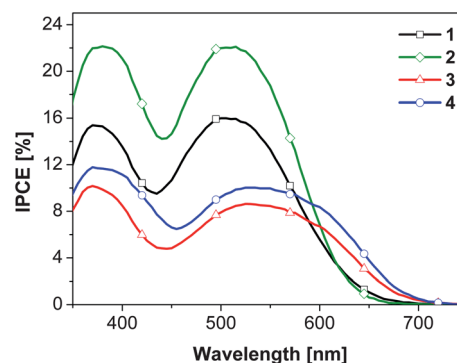


Fig. 6 Incident photon to charge carrier conversion efficiencies for devices constructed using dyes **1**–**4**.

maximum of only about 8% at 533 nm, which is slightly increased to 10% for ethynylene-containing regioisomeric dye **4**. The results clearly show the influence of the ethynylene spacer on the solar cell performance. In addition to the increasing magnitude of the IPCE response, there is also an observed broadening in the absorption peak corresponding to high energy absorption (~ 400 to 450 nm), which is in agreement with the thin film absorption spectra seen in Fig. 1b.

The IPCE responses show that, in spite of the improved light harvesting, and a similar magnitude of light absorption (Fig. 1b), lower quantum efficiencies for either charge injection or transport are mostly responsible for the smaller J_{SC} values recorded for dyes **3** and **4**. This might be due to the planarization of the perylene–thiophene unit. In Fig. 1b it can be seen that in all cases spectra of the dyes on NiO films show a peak at ~ 350 to 360 nm which is higher than the one at ~ 500 nm. In contrast, the peaks of the IPCE at both wavelength regions for all devices are nearly identical. In these p-DSC devices the IPCE response at short wavelengths is mitigated due to the light harvesting competition from both the electrolyte and NiO.

Transient absorption spectroscopy

Transient absorption spectroscopy (TAS) experiments of dyes **1–4** on NiO films in the absence of a redox mediator were performed to investigate the recombination kinetics of the photo-reduced dye anions with holes in the NiO-photocathode (Fig. 7). Substantially higher signal magnitudes have been measured for dyes **1** and **2** compared to the regioisomeric dyes **3** and **4**, which cannot be attributed to differences in the absorbed pump beam intensity ($1-10^{-\text{ad}}$, where ad is the optical density of the films) at the pump wavelength of 532 nm (see Fig. 1b and S1†), since the optical densities of the films were nearly identical. Furthermore, the absorbance of the electrochemically reduced dye species in DMF solution is also very similar at the probe wavelength of 700 nm (see Fig. S2†). While the electrochemically reduced **3** and **4** absorb less light in the 600–700 nm main anion absorption band, the anions of **3** and **4** absorb slightly more due to their red-shifted absorbance band at the 700 nm TA probe wavelength. Therefore, the reduced TAS signal magnitude in Fig. 7 is not due to a lower absorption coefficient of the **3** and **4** anions, but rather originates from reduced hole injection yield and/or a fast

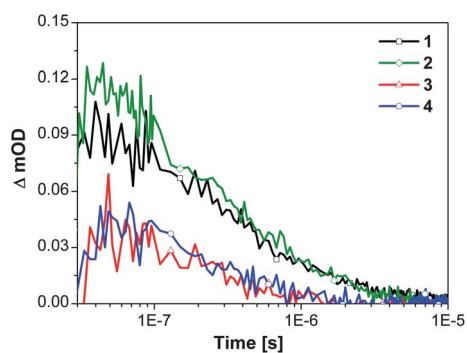


Fig. 7 Transient absorption decay signals of NiO films sensitized with **1–4** after laser excitation at a wavelength of 532 nm (intensity: $32 \mu\text{J cm}^{-2} \text{ pulse}^{-1}$), probing at 700 nm.

component of the recombination kinetics, beyond the time resolution of our setup (50 ns).

The transient spectra of photo-reduced dyes **1** and **3** resemble that of the electrochemically generated species (Fig. 8a and b as well as Fig. S2†). We note that the intense absorption peak of the electrochemically generated anion **3** centred at 625 nm is not evident in the TA spectrum (Fig. 8b). We attribute this to the stronger overlap of the red-shifted ground state absorption of **3** and the first absorption peak of the anion, which has not shifted significantly between **1** and **3**. As a result TAS of NiO sensitized with dye **3** shows a less significant absorption feature in the 600–650 nm wavelength range than NiO films sensitized with dye **1**. The NiO hole–dye anion recombination kinetics for all dyes in Fig. 7 are quite similar and can be characterized with a signal decay half time of around 300 ns for **1** and **2** and around 250 ns for **3** and **4**, which is very similar to our previously reported value for the dye **1**.¹⁸ Contrary to our expectation, the elongation of the π -bridge in dyes **2** and **4** using the ethynyl spacer did not translate into an improved dye anion lifetime compared to **1** and **3**. In our previous study, increasing the number of bithiophene units resulted in a 7-fold increase for the quaterthiophene and a further 2 fold increase for the sexithiophene bridge.¹⁸ Clearly, the ethynyl linker is found to be not as effective as the bithiophene bridge. A possible explanation for the reduced charge generation yield in **3** and **4** could be the reduction of the torsion angle between the PMI and the adjacent thiophene unit, thus resulting in a faster hole–dye anion recombination rate.

Further work should focus on determining the photophysical origin of the reduced performance of dyes **3** and **4** using sub-ns time-resolved photoluminescence and transient absorption spectroscopy. Furthermore, photo-reduced dye anion and NiO recombination is fast for all four dyes, competing with dye anion

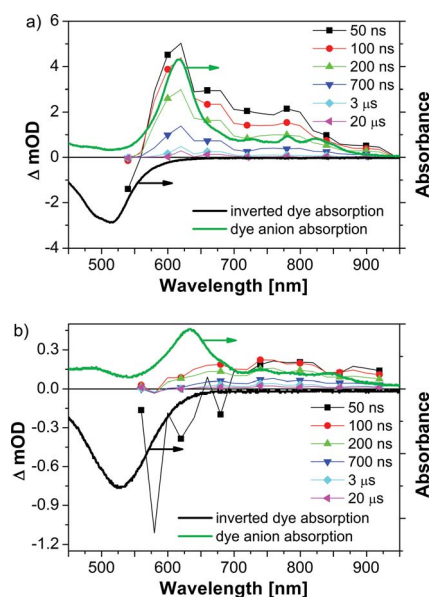


Fig. 8 Transient absorption spectrum of NiO films sensitized with **1** (a) and **3** (b) after laser excitation at a wavelength of 532 nm (intensity: $90 \mu\text{J cm}^{-2} \text{ pulse}^{-1}$). The green solid line represents scaled absorption of electrochemically reduced (at -550 mV versus Ag/AgCl) dye anion in DMF. The thick black line represents scaled and inverted absorption spectrum of neutral dye in DMF at open circuit.

regeneration occurring on a similar time scale. Extending dye anion lifetime to the μs to ms time range, similarly to frequently observed long photooxidized dye–TiO₂ lifetimes of most n-type dye-sensitized photoanodes, will be crucial for photocathodes to match their performance, a prerequisite for high efficiency tandem (np-DSC) devices.

Conclusion

Synthesis and characterization of a new series of PMI–2T–TPA triads have been reported where (1) an ethynyl group was used to extend the π -bridge length, and/or (2) the positions of the hexyl chains on the thiophenes that comprise the π -bridge were altered. Subsequently, steric hindrances within the dye were investigated. Optical, electrochemical and device results showed the benefit of an ethynyl linker, although this was much more pronounced for dye **2** compared to **1** than for **4** compared to **3**. There were also clearly observed differences for the regioisomeric dyes **3** and **4** compared to dyes **1** and **2**. Quantum-chemical DFT calculations showed the planarization of the perylene–thiophene linkage for compounds **3** and **4**, resulting in a beneficial red shift (greater light harvesting ability), however, this was outweighed by a decreased charge generation and/or collection, suggesting that torsion between the acceptor and donor may be necessary for high quantum efficiencies. A broad IPCE spectrum is observed for these dyes in the spectral region between 350 and 700 nm, which increases by insertion of an acetylene unit leading to an increased π -conjugation length. Using 1.5 μm thick mesoporous NiO films, power conversion efficiencies in the range from 0.04 to 0.10% under full sun illumination (simulated AM 1.5G sunlight, 100 mW cm⁻²) were observed, which give valuable insight into the construction principles of dyes for NiO-photocathodes useful for p-DSCs. It should be noted that with dye **2** comprising an ethynylene spacer the power conversion efficiency of the original PMI–2T–TPA **1** has been increased from 0.08 to 0.10%, *i.e.* a 25% improvement. Furthermore, to develop high performance tandem devices it is also crucial to develop p-type sensitizers that match the performance of their n-type counterpart and should have complementary absorption, work towards this direction is in progress.

Experimental

General procedures

¹H NMR spectra were recorded in CDCl₃ and d⁶-DMSO on a Bruker AMX 400 at 400 MHz. ¹³C NMR spectra were recorded in CDCl₃ and d⁶-DMSO on a Bruker AMX 400 at 100 MHz. Chemical shifts are denoted by a δ unit (ppm). The splitting patterns are designated as follows: s (singlet), d (doublet), t (triplet), dt (double triplet), quin (quintet), hep (heptet) and m (multiplet) and the assignments are *Pery* (perylene), *TPA* (triphenylamine), *Ph* (phenyl), and *Th* (thiophene) for ¹H NMR. Mass spectra were recorded with a Varian Saturn 2000 GC-MS and with a MALDI-TOF MS Bruker Reflex 2 (dithranol as the generally used matrix and 2,5-dihydroxybenzoic acid for the free acids). Melting points were determined with a Büchi B-545 melting point apparatus and are not corrected. Gas chromatography was carried out using a Varian CP-3800 gas chromatograph. HPLC analyses were performed on a Shimadzu

SCL-10A equipped with a SPD-M10A photodiode array detector and a SC-10A solvent delivery system using a *LiChrospher* column (Silica 60, 5 μm , Merck). Thin-layer chromatography was carried out on Silica Gel 60 F₂₅₄ aluminium plates (Merck). Solvents and reagents were purified and dried by usual methods prior to use and typically used under inert gas atmosphere. The following starting materials were purchased and used without further purification: *p*-bromobenzoic acid (Merck), thionyl chloride (Merck), potassium *tert*-butylate (Merck), iodine monochloride (Merck), zinc acetate (Merck), bis(pinacolato)diboron (Lancaster), ethynyl-trimethyl-silane (ABCR), and Pd(dppf)Cl₂ (Aldrich).

Optical and cyclic voltammetric measurements

UV-Vis spectra in dichloromethane solution were taken on a Perkin-Elmer Lambda 19 spectrometer. Thin film spectra were taken using a Varian Cary 5000 spectrometer with integrating sphere attachment (Varian Internal DRA 2500). Cyclic voltammetry experiments were performed with a computer-controlled EG&G PAR 273 potentiostat in a three-electrode single-compartment cell (5 mL). The platinum working electrode consisted of a platinum wire sealed in a soft glass tube with a surface of $A = 0.785 \text{ mm}^2$, which was polished down to 0.5 μm with Buehler polishing paste prior to use in order to obtain reproducible surfaces. The counter electrode consisted of a platinum wire and the reference electrode was an Ag/AgCl reference electrode. All potentials were internally referenced to the ferrocene/ferricenium couple. For the measurements concentrations of 10⁻³ mol L⁻¹ of the electroactive species were used in freshly distilled and deaerated dichloromethane (*LiChrosolv*, Merck) and 0.1 M tetrabutylammonium hexafluorophosphate (TBAPF₆, Fluka) which was twice recrystallized from ethanol and dried under vacuum prior to use.

Quantum-chemical calculations

Density functional theory was employed with the hybrid functionals B3LYP and the basis set 6-31G⁺ including d and p diffuse functions from the Gaussian 09 package. The long hexyl chains, which have no significant impact on the frontier orbitals of the chromophores, were replaced with ethyl substituents in order to accelerate the convergence of optimizations.

Device fabrication

4 × 4 mm NiO films were screen printed onto F:SnO₂ glass (Nippon Sheet Glass) using a paste produced by grinding 15 g of NiO (Inframmat) in ethanol, added in small aliquots. 50 mL of a 10 wt% ethyl cellulose solution in ethanol and 100 mL terpineol were then added and after mixing ethanol was evaporated to leave a terpineol based paste. These were sintered for 30 minutes at 400 °C, then 10 minutes at 550 °C, before being immersed into dye solutions (0.2 mM in DMF) for 2 hours. Films were then removed from this dye solution and rinsed subsequently in DMF and ethanol before being allowed to dry. Counter electrodes were produced by applying one drop of H₂PtCl₆ (10 mM in ethanol) to F:SnO₂ glass and thermally decomposing by firing at 400 °C for 15 minutes under a gentle flow of air. Counter and working electrodes were sandwiched together with a 25 μm Surlyn

(Dupont) spacer, and heated to ~ 120 °C for ~ 30 seconds in order to create a seal. The electrolyte solution was introduced through a pre-drilled hole in the counter electrode, which was subsequently sealed with another piece of Surlyn and a microscope cover slip.

Current–voltage characterisation

Solar cells were tested using simulated sunlight (AM1.5, 1000 W m^{-2}) provided by an Oriel solar simulator with an AM1.5 filter. Current–voltage characteristics were measured using a Keithley 2400 source meter. Cells were biased from high to low, with 10 mV steps and a 250 ms settling time between the application of a bias and current measurement.

Incident photon to current efficiency characterisation

IPCE was measured with the cell held under short circuit conditions and illuminated by monochromatic light. A Cornerstone 260 monochromator was used in conjunction with an optical fibre, Keithly 2400 source meter and 150 W Oriel Xe lamp. Prior to testing a 30 second 'rest' period was introduced to ensure the dark current dropped to zero when the cell was short circuited. Additionally, 200 ms settling time was applied between the monochromator switching to a wavelength and measurement commencing, which was followed by an averaged reading over a 1 second period.

Transient absorption spectroscopy

TAS experiments were performed as previously reported.³² A 532 nm pump was used (Nd-YAG, INDI-40-10, Spectra-Physics), operating in Q-switch mode (6 ns pulse) at a 10 Hz repetition rate. A 1000 W Xe lamp (Edinburgh Instruments) was used for the probe, employing a 700 nm bandpass filter with an FWHM of 40 nm. The signal was passed through a monochromator to a Si detector (Femto), and a signal recorded by a Tektronix 4054 oscilloscope.

Synthesis

4-Bromo-benzoic acid *tert*-butyl ester (6).²⁴ 4-Bromobenzoic acid **5** (10.1 g, 50 mmol) was added to 25 mL thionyl chloride. After three drops of DMF were added to the suspension it was stirred under reflux for one hour. When the reaction was completed the excess of thionyl chloride was removed in vacuum. The residual yellowish solid **5a** was dissolved in 10 mL dry THF and the resulting solution was cooled down to 0 °C. Next, under constant stirring a solution of potassium *tert*-butylate (6.7 g, 60 mL) dissolved in 50 mL dry THF was added slowly over a period of one hour while the temperature was not allowed to exceed 5 °C. The resulting suspension was poured into 250 mL water and was extracted with diethylether. The organic phase was washed with a saturated sodium hydrogen carbonate solution and was dried with magnesium sulfate. After the solvent was removed by rotary evaporation the crude product was purified by bulb-to-bulb distillation to afford ester **6** (11.2 g, 87%) as a colorless liquid. ¹H NMR (400 MHz, CDCl₃): δ = 7.84 (d, *J* = 8.6 Hz, 2H, *Ph-2H,6H*), 7.54 (d, *J* = 8.6 Hz, 2H, *Ph-3H,5H*), 1.59 (s, 9H, C-(CH₃)₃); ¹³C NMR (100 MHz, CDCl₃): 165.38, 132.03,

131.06, 131.50, 128.00, 81.84, 28.74; MS (EI) *m/z*: [M]⁺ calcd for C₁₁H₁₃BrO₂, 256; found, 257.

4-(*N*-Phenylamino)benzoic acid *tert*-butyl ester (7). Aniline (1.4 g, 15 mmol) and ester **6** (2.6 g, 10 mmol) were dissolved in 50 mL dry toluene. After the solution was degassed potassium *tert*-butylate (2.5 g, 22.5 mmol) and the catalyst (Pd₂dba₃ [104 mg, 0.1 mmol] and [HP(*t*-Bu₃)]BF₄ [46 mg, 0.16 mmol]) were added. Next, the resulting suspension was degassed and stirred for 2 hours at room temperature. After the reaction was completed it was poured into water and the aqueous phase was acidified with hydrochloric acid. The water phase was extracted with dichloromethane and the organic phase was dried with magnesium sulfate. After the solvent was removed by rotary evaporation the residue was dissolved in dichloromethane and was filtered over a short silica column to remove the catalytic residues. The solvent was evaporated and the crude product was dissolved in 5 mL hot chloroform. After addition of 50 mL hot *n*-hexane the product was allowed to crystallize. The white crystals of **7** (2.1 g, 78%) were filtered off and dried in vacuum. M.p.: 115 °C; ¹H NMR (400 MHz, CDCl₃): δ = 7.89–7.85 (m, 2H, (*t*-Bu)OOC-*Ph-2H,6H*), 7.35–7.28 (m, 2H, *Ph-2H,6H*), 7.17–7.13 (m, 2H, (*t*-Bu)OOC-*Ph-3H,5H*), 7.04 (d, *J* = 7.4 Hz, 1H, *Ph-4H*), 7.00–6.95 (m, 2H, *Ph-3H,5H*), 5.99 (s, 1H, -NH), 1.58 (s, 9H, C-(CH₃)₃); ¹³C NMR (100 MHz, CDCl₃): δ = 165.75, 147.54, 141.18, 131.27, 129.48, 123.28, 122.83, 120.06, 114.75, 80.25, 28.31; MS (EI) *m/z*: [M]⁺ calcd for C₁₇H₁₉NO₂, 269; found, 269. Elemental analysis: calcd (%) for C₁₇H₁₉NO₂: C 75.81, H 7.11, N 5.20; found C 75.85, H 7.00, N 5.19%.

***N,N*-Di(4-benzoic acid *tert*-butyl ester)phenylamine (8).** Diphenylamine **7** (0.97 g, 3.6 mmol) and ester **6** (1.0 g, 3.9 mmol) were dissolved in 18 mL dry toluene. After the solution was degassed potassium *tert*-butylate (807 mg, 7.5 mmol) and the catalyst (Pd₂dba₃ [37 mg, 36 μ mol] and [HP(*t*-Bu₃)]BF₄ [17 mg, 58 μ mol]) were added. Next, the resulting suspension was degassed and was stirred for 2 hours at room temperature. After the reaction was completed it was poured into water and the aqueous phase was acidified with hydrochloric acid (pH = 7). The water phase was extracted with dichloromethane and the organic phase was dried with magnesium sulfate. After the solvent was removed by rotary evaporation the crude product was purified by column chromatography (SiO₂, dichloromethane : petrol ether [2 : 1]) to give **8** (1.5 g, 93%) as a white solid. M.p.: 63 °C; ¹H NMR (400 MHz, CDCl₃): δ = 7.86 (d, *J* = 8.8 Hz, 4H, (*t*-Bu)OOC-*Ph-2H,6H*), 7.32 (d, *J* = 7.8 Hz, 2H, *Ph-2H,6H*), 7.17 (d, *J* = 7.3 Hz, 1H, *Ph-4H*), 7.14–7.10 (m, 2H, *Ph-3H,5H*), 7.06 (d, *J* = 8.8 Hz, 4H, (*t*-Bu)OOC-*Ph-3H,5H*), 1.58 (s, 18H, C-(CH₃)₃); ¹³C NMR (100 MHz, CDCl₃): δ = 165.40, 150.76, 130.80, 129.75, 126.31, 126.10, 122.43, 80.70, 28.26; MS (CI) *m/z*: [M]⁺ calcd for C₂₈H₃₁NO₄, 445; found, 445. Elemental analysis: calcd (%) for C₂₈H₃₁NO₄: C 75.48, H 7.01, N 3.14; found C 75.40, H 7.03, N 3.05%.

***N,N*-Di(4-benzoic acid *tert*-butyl ester)-4-iodo-phenylamine (9).** Iodine chloride (413 mg, 2.46 mmol) and zinc acetate (270 mg, 1.23 mmol) were added to 3 mL dioxane and was stirred for 15 min at room temperature. Next, diphenylamine **8** (550 mg, 1.23 mmol) dissolved in 2 mL dioxane was added slowly and the

resulting brownish solution was stirred at room temperature for 3 hours. After the reaction was completed the reaction mixture was poured into 20 mL of a 1 molar sodium thiosulfate solution. The water phase was extracted with dichloromethane and the organic phase was dried with magnesium sulfate. After the solvent was removed by rotary evaporation the crude product was dissolved in 3 mL hot chloroform. After addition of 30 mL hot methanol the product was allowed to crystallize. The white crystals of **9** (635 mg, 90%) were filtered off and dried in vacuum. M.p.: 172–173 °C; ¹H NMR (400 MHz, CDCl₃): δ = 7.87 (d, *J* = 8.8 Hz, 4H, (*t*-Bu)OOC-*Ph*-2*H*,6*H*), 7.60 (d, *J* = 8.8 Hz, 2H, *Ph*-3*H*,5*H*), 7.05 (d, *J* = 8.8 Hz, 4H, (*t*-Bu)OOC-*Ph*-3*H*,5*H*), 6.87 (d, *J*₁ = 8.8 Hz, 2H, *Ph*-2*H*,6*H*), 1.58 (s, 18H, C-(CH₃)₃); ¹³C NMR (100 MHz, CDCl₃): δ = 126.26, 150.23, 138.72, 130.92, 127.57, 126.64, 122.78, 80.86, 28.23; MS (MALDI-TOF) *m/z*: [M]⁺ calcd for C₂₈H₃₀INO₄, 571; found [M + H]⁺, 572. Elemental analysis: calcd (%) for C₂₈H₃₀INO₄: C 58.85, H 5.29, N 2.45; found C 58.92, H 5.32, N 2.37%.

***N,N*-Di(4-benzoic acid *tert*-butyl ester)-4-trimethylsilyl-ethynyl-phenylamine (10).** Triphenylamine **9** (115 mg, 0.2 mmol), ethynyl-trimethylsilane (30 mg, 0.3 mmol), Pd(PPh₃)₂Cl₂ (7.0 mg, 0.01 mmol) and CuI (3.8 mg, 0.02 mmol) were added to 0.5 mL piperidine. The reaction mixture was carefully degassed and was stirred at 60 °C for 3–4 hours. After the reaction was completed the mixture was poured into water (20 mL) and was acidified with concentrated hydrochloric acid (pH = 1). The organic layer was taken off while the water phase was extracted with dichloromethane. The combined organic phases were dried with magnesium sulfate and the solvent was removed by rotary evaporation. The crude product was purified by column chromatography (SiO₂/dichloromethane : petrol ether [2 : 1]) to give **10** (100 mg, 92%) as a white solid. M.p.: 150–151 °C; ¹H NMR (400 MHz, CDCl₃): δ = 7.87 (d, *J* = 8.6 Hz, 4H, (*t*-Bu)OOC-*Ph*-2*H*,6*H*), 7.39 (d, *J* = 8.6 Hz, 2H, *Ph*-3*H*,5*H*), 7.07 (d, *J* = 8.6 Hz, 4H, (*t*-Bu)OOC-*Ph*-3*H*,5*H*), 7.02 (d, *J* = 8.6 Hz, 2H, *Ph*-2*H*,6*H*), 1.58 (s, 18H, C-(CH₃)₃), 0.25 (s, 9H, Si-(CH₃)₃); ¹³C NMR (100 MHz, CDCl₃): δ = 165.26, 150.25, 146.43, 133.32, 130.89, 126.72, 124.86, 123.06, 118.89, 104.60, 94.41, 80.84, 28.22; MS (MALDI-TOF) *m/z*: [M]⁺ calcd for C₃₃H₃₉NO₄Si, 541; found [M + H]⁺, 542. Elemental analysis: calcd (%) for C₃₃H₃₉NO₄Si: C 73.16, H 7.26, N 2.59; found C 72.89, H 7.17, N 2.39%.

***N,N*-Di(4-benzoic acid *tert*-butyl ester)-4-ethynyl-phenylamine (11).** To a solution of diphenylamine **10** (65 mg, 0.12 mmol) in 1 mL THF was added caesium fluoride (54 mg, 0.36 mmol dissolved in 0.36 mL methanol). The resulting solution was stirred for 1 hour at room temperature. After the reaction was completed the mixture was poured into water and the organic layer was taken off while the water phase was extracted with dichloromethane. The combined organic phases were washed with water three times and were dried with magnesium sulfate. The solvent was removed in vacuum to give **11** (56 mg, quantitative) as a brownish, viscous oil which was used without further purification. ¹H NMR (400 MHz, CDCl₃): δ = 7.87 (d, *J* = 8.6 Hz, 4H, (*t*-Bu)OOC-*Ph*-2*H*,6*H*), 7.41 (d, *J* = 8.6 Hz, 2H, *Ph*-3*H*,5*H*), 7.07 (d, *J* = 8.6 Hz, 4H, (*t*-Bu)OOC-*Ph*-3*H*,5*H*), 7.04 (d, *J* = 8.6 Hz, 2H, *Ph*-2*H*,6*H*), 3.07 (s, 1H, C≡CH), 1.58 (s, 18H, C-(CH₃)₃); ¹³C NMR (100 MHz, CDCl₃): δ = 165.41, 150.39,

146.94, 133.63, 131.07, 127.01, 125.00, 123.30, 117.93, 107.90, 83.40, 81.02, 28.38; 165.26, 150.25, 146.43, 133.32, 130.89, 126.72, 124.86, 123.06, 118.89, 104.60, 94.41, 80.84, 28.22; MS (CI) *m/z*: [M]⁺ calcd for C₃₀H₃₁NO₄, 469; found [M + H]⁺, 470.

5-Trimethylsilyl-4,3'-dihexyl-2,2'-bithiophene (13). *n*-Butyllithium (0.39 mL, 0.62 mmol) was added dropwise to a solution of bromo-bithiophene **12** (250 mg, 0.60 mmol) in 3 mL dry THF at –78 °C. After the addition the solution was stirred for 15 min at –78 °C. Trimethylsilyl chloride was added, subsequently. The cooling bath was removed and the reaction was stirred until it had warmed up to room temperature. Then the mixture was poured into water and the organic layer was separated and the aqueous phase was extracted with diethylether. The combined organic phases were washed with brine and dried over sodium sulfate and the solvent was removed by rotary evaporation. The crude product was purified by column chromatography (SiO₂/*n*-hexane) to give **13** (203 mg, 83%) as a yellow oil. ¹H NMR (400 MHz, CDCl₃): δ = 7.13 (d, *J* = 5.2 Hz, 1H, 5'-*H*), 7.03 (s, 1H, 3-*H*), 6.91 (d, *J* = 5.2 Hz, 4'-*H*), 2.75 (t, *J* = 7.9 Hz, 2H, α'-CH₂), 2.64 (t, *J* = 7.9 Hz, 2H, α-CH₂), 1.66–1.57 (m, 4H, β-CH₂, β'-CH₂), 1.41–1.26 (m, 12H, -CH₂-), 0.90 (t, *J* = 6.8 Hz, 3H, Th'-CH₃), 0.88 (t, *J* = 6.7, 3H, Th-CH₃), 0.35 (s, 9H, Si-CH₃); ¹³C NMR (100 MHz, CDCl₃): δ = 150.672, 140.044, 139.164, 132.879, 130.974, 129.921, 129.133, 123.293, 31.761, 31.721, 31.639, 31.451, 30.629, 29.398, 29.183, 22.623, 14.097, 0.401; MS (EI) *m/z*: [M]⁺ calcd for C₂₃H₃₈S₂Si, 406; found, 406. Elemental analysis: calcd (%) for C₂₃H₃₈S₂Si: C 67.91, H 9.42, S 15.77; found C 68.18, H 9.40, S 15.56%.

5-(4,3'-Dihexyl-5'-trimethylsilyl-2,2'-bithien-5-yl)-4,4,5,5-tetramethyl-[1,3,2]dioxaborolane (14). *n*-Butyllithium (0.14 mL, 0.35 mmol) was added dropwise to a solution of trimethylsilyl-bithiophene **13** (130 mg, 0.32 mmol) in 1.5 mL dry THF at –78 °C. After the addition the solution was stirred for 15 min at –78 °C. Trimethylsilyl chloride was added, subsequently. The cooling bath was removed and the reaction was stirred until it had warmed up to room temperature. Then the mixture was poured into water and the organic layer was separated and the aqueous phase was extracted with diethylether. The combined organic phases were washed with brine and dried over sodium sulfate and the solvent was removed by rotary evaporation. Boronic ester **14** was obtained as a yellow oil (165 mg, 92%) with a purity of 95% (GC). It was used without further purification. ¹H NMR (400 MHz, CDCl₃): δ = 7.44 (s, 1H, 4-*H*), 7.10 (s, 1H, 3'-*H*), 2.75 (t, *J* = 7.9 Hz, 2H, α'-CH₂), 2.64 (t, *J* = 7.9 Hz, 2H, α-CH₂), 1.66–1.57 (m, 4H, β-CH₂, β'-CH₂), 1.41–1.26 (m, 12H, -CH₂-), 0.90 (t, *J* = 6.8 Hz, 3H, Th'-CH₃), 0.88 (t, *J* = 6.7, 3H, Th-CH₃), 0.35 (s, 9H, Si-CH₃); MS (EI) *m/z*: [M]⁺ calcd for C₂₉H₄₉BO₂S₂Si, 532; found, 533.

5-([*N*-(2,6-Diisopropylphenyl)]-9-perylenyl-3,4-dicarboximide)-3,4'-dihexyl-2,2'-bithiophene (16). Bromoperylene **15** (187 mg, 0.32 mmol) and bithiophene boronic ester **14** (226 mg, 0.38 mmol) were dissolved in 3 mL DME. The resulting solution was carefully degassed and the catalyst (Pd(PPh₃)₄ (4 mol%) and the base (2 M aqueous potassium phosphate solution (0.48 mL, 3 eq.)) were added. Next, the reaction mixture was carefully degassed and stirred at 80 °C for 1.5 h. Then

tetrabutylammonium fluoride (400 mg, 1.27 mmol) was added and the reaction mixture was stirred for a further 2.5 h. After the reaction was completed the mixture was poured into water (15 mL) and the organic layer was separated while the aqueous phase was extracted with dichloromethane. The combined organic phases were dried over sodium sulfate and the solvent was removed by rotary evaporation. The crude product was purified by column chromatography (SiO₂/dichloromethane : *n*-hexane [2 : 1]) to give **16** (238 mg, 92%) as a red solid. M.p.: 94–96 °C; ¹H NMR (400 MHz, CDCl₃): δ = 8.65–8.62 (m, 2H, *Pery-1H,6H*), 8.49–8.36 (m, 5H, *Pery-2H,5H,7H,8H,12H*), 7.71 (d, *J* = 7.9 Hz, *Pery-10H*), 7.64 (t, *J* = 8.0 Hz, 1H, *Pery-11H*), 7.49 (t, *J* = 7.7 Hz, 1H, *Ph-4H*), 7.36 (d, *J* = 7.8 Hz, 2H, *Ph-3H,5H*), 7.18 (s, 1H, *Th-4H*), 7.07 (d, *J* = 0.9, 1H, *Th'-5H*), 6.96 (d, *J* = 0.9, 1H, *Th'-3H*), 2.87 (t, *J* = 7.7 Hz, 2H, *Th-α'-CH₂*), 2.84–2.74 (m, 2H, *Ph-CH-(CH₃)₂*), 2.65 (t, *J* = 7.6 Hz, 2H, *Th-α'-CH₂*), 1.79–1.64 (m, 4H, *Th-β-CH₂*, *Th-β'-CH₂*), 1.49–1.29 (m, 12H, *-CH₂-*), 1.20 (d, *J* = 6.8 Hz, 12H, *Ph-CH-(CH₃)₂*), 0.91 (t, *J* = 7.0 Hz, 6H, *Th-CH₃*, *Th'-CH₃*); ¹³C NMR (100 MHz, CDCl₃): δ = 163.92, 145.64, 143.80, 139.98, 138.33, 137.49, 137.18, 135.37, 135.21, 132.76, 132.36, 131.98, 131.28, 131.01, 130.43, 129.42, 129.29, 129.07, 128.80, 128.64, 128.44, 127.51, 127.26, 126.74, 124.04, 124.00, 123.36, 120.88, 120.82, 120.40, 120.28, 120.10, 31.69, 30.71, 30.51, 30.41, 29.43, 29.30, 29.14, 29.02, 24.02, 22.66, 14.11; MS (MALDI-TOF) *m/z*: [M]⁺ calcd for C₅₄H₅₅NO₂S₂, 813; found [M + H]⁺, 814. Elemental analysis: calcd (%) for C₅₄H₅₅NO₂S₂: C 79.66, H 6.81, N 1.72; found C 79.66, H 6.61, N 1.80%.

5-([N-(2,6-Diisopropylphenyl)]-9-perylenyl-3,4-dicarboximide)-3,4'-dihexyl-5'-iodo-2,2'-bithiophene (18). To a solution of perylenyl-bithiophene **16** (230 mg, 0.28 mmol) in dry dichloromethane was added mercury caproate (122 mg, 0.28 mmol). The resulting suspension was stirred at room temperature for 24 h until the mercury compound was completely dissolved. Next, iodine (1.1 equivalents) was added and the mixture was stirred for another 6 h. Then the solution was filtered over basic aluminium oxide and the filtrate was concentrated in vacuum. Upon addition of methanol the product was allowed to precipitate, filtered and dried in vacuum to give **17** (245 mg, 92%) as a red solid. M.p.: 98–100 °C; ¹H NMR (400 MHz, CDCl₃): δ = 8.68–8.65 (m, 2H, *Pery-1H,6H*), 8.53–8.44 (m, 5H, *Pery-2H,5H,7H,8H,12H*), 7.73 (d, *J* = 7.8 Hz, *Pery-10H*), 7.69 (t, *J* = 8.0 Hz, 1H, *Pery-11H*), 7.49 (t, *J* = 7.8 Hz, 1H, *Ph-4H*), 7.35 (d, *J* = 7.8 Hz, 2H, *Ph-3H,5H*), 7.18 (s, 1H, *Th-4H*), 6.87 (s, 1H, *Th'-3H*), 2.85–2.75 (m, 5H, *Th'-α-CH₂*, *Ph-CH-(CH₃)₂*), 2.58 (t, *J* = 7.7 Hz, 2H, *Th-α-CH₂*), 1.77–1.59 (m, 4H, *Th-β-CH₂*, *Th'-β-CH₂*), 1.49–1.28 (m, 12H, *-CH₂-*), 1.19 (d, *J* = 6.9 Hz, 12H, *Ph-CH-(CH₃)₂*), 0.91 (t, *J* = 6.9 Hz, 6H, *Th-CH₃*, *Th'-CH₃*); ¹³C NMR (100 MHz, CDCl₃): δ = 163.96, 147.79, 145.73, 140.58, 140.23, 139.00, 137.58, 137.27, 135.20, 132.54, 132.07, 131.83, 131.25, 131.06, 130.55, 129.52, 129.42, 129.03, 129.00, 128.96, 128.60, 127.43, 126.92, 126.79, 124.15, 124.00, 123.39, 121.09, 120.47, 120.30, 74.46, 32.38, 31.66, 30.70, 29.98, 29.45, 29.26, 29.16, 28.92, 24.01, 22.65, 22.62, 14.09; MS (MALDI-TOF) *m/z*: [M]⁺ calcd for C₅₄H₅₄INO₂S₂, 939; found [M + H]⁺, 940. Elemental analysis: calcd (%) for C₅₄H₅₄INO₂S₂: C 69.00, H 5.74, N 1.49; found C 69.18, H 5.64, N 1.63%.

Di-tert-butyl 4,4'-[(4-({5'-([N-(2,6-diisopropylphenyl)]-9-perylenyl-3,4-dicarboximide)-3',4'-dihexyl-2,2'-bithien-5-yl}ethynyl)phenyl)imino]dibenzoate (19). Iodinated perylenyl-bithiophene **17** (45 mg, 48 μmol), triphenylamine **11** (27 mg, 57 μmol) and CuI (10 mol%) were dissolved in 1.5 mL toluene. The solution was carefully degassed and the catalyst (Pd(PPh₃)₂Cl₂ (4 mol%)) and 0.9 mL diisopropylamine were added. The resulting solution was degassed carefully and stirred at room temperature for 4 h. After the reaction was completed the mixture was poured into water (7 mL) and the organic layer was separated while the aqueous phase was extracted with dichloromethane. The combined organic phases were dried over sodium sulfate and the solvent was removed by rotary evaporation. The crude product was purified by column chromatography (SiO₂/*n*-hexane : ethyl acetate [5 : 1]) to give **19** (37 mg, 60%) as a dark red solid. M.p.: 170–171 °C; ¹H NMR (400 MHz, CDCl₃): δ = 8.68–8.65 (m, 2H, *Pery-1H,6H*), 8.52–8.43 (m, 5H, *Pery-2H,5H,7H,8H,12H*), 7.90 (d, *J* = 8.7 Hz, 4H (*t*-Bu)OOC-*Ph-2H,6H*), 7.74 (d, *J* = 7.8 Hz, 1H, *Pery-10H*), 7.69 (t, *J* = 8.0 Hz, 1H, *Ph-4H*), 7.50–7.44 (m, 3H, *Pery-11H*, *Ph-3H,5H*), 7.35 (d, *J* = 7.8 Hz, 2H, *Ph-3H,5H*), 7.19 (s, 1H, *Th-3H*), 7.12–7.09 (m, 6H, (*t*-Bu)OOC-*Ph-3H,5H*, *TPA-Ph-2H,6H*), 7.03 (s, 1H, *Th'-4H*), 2.89 (t, *J* = 7.8 Hz, 2H, *Th'-α-CH₂*), 2.84–2.74 (m, 2H, *Ph-CH-(CH₃)₂*, *Th-α-CH₂*), 1.80–1.69 (m, 4H, *Th-β-CH₂*, *Th'-β-CH₂*), 1.60 (s, 18H, *t*Bu-*CH₃*), 1.50–1.28 (m, 12H, *-CH₂-*), 1.20 (d, *J* = 6.8 Hz, 12H, *Ph-CH-(CH₃)₂*), 0.92 (t, *J* = 7.2 Hz, 3H, *Th'-CH₃*), 0.90 (t, *J* = 7.0 Hz, 3H, *Th-CH₃*); ¹³C NMR (100 MHz, CDCl₃): δ = 165.28, 163.96, 150.28, 148.34, 146.34, 145.75, 140.69, 138.95, 137.57, 137.25, 135.79, 135.20, 132.61, 132.53, 132.17, 132.07, 131.54, 131.09, 130.95, 130.55, 129.51, 128.99, 128.96, 128.60, 127.44, 127.06, 126.90, 126.87, 125.04, 124.15, 124.02, 123.40, 123.16, 121.09, 121.07, 120.47, 120.30, 118.96, 118.48, 96.34, 82.55, 80.89, 31.71, 31.68, 30.66, 30.21, 29.72, 29.68, 29.34, 29.18, 29.00, 28.26, 24.03, 22.68, 22.64, 14.13, 14.11; MS (MALDI-TOF) *m/z*: [M]⁺ calcd for C₈₄H₈₄N₂O₆S₂, 1281; found [M + H]⁺, 1282. Elemental analysis: calcd (%) for C₈₄H₈₄N₂O₆S₂: C 78.72, H 6.61, N 2.19; found C 78.86, H 6.72, N 2.23%.

Di-tert-butyl 4,4'-[(4-({5'-([N-(2,6-diisopropylphenyl)]-9-perylenyl-3,4-dicarboximide)-3',4'-dihexyl-2,2'-bithien-5-yl}ethynyl)phenyl)imino]dibenzoate (20). Iodinated perylenyl-bithiophene **18** (94 mg, 0.1 mmol), triphenylamine **11** (56 mg, 0.12 mmol) and CuI (10 mol%) were dissolved in 1 mL piperidine. The solution was carefully degassed and the catalyst (Pd₂(dba)₃ [2.5 mol%] and [HP(*t*-Bu)₃]BF₄ [10 mol%]) were added. The resulting solution was degassed carefully and stirred at room temperature for 24 h. After the reaction was completed the mixture was poured into water and the organic layer was separated while the aqueous phase was extracted with dichloromethane. The combined organic phases were dried over magnesium sulfate and the solvent was removed by rotary evaporation. The crude product was purified by column chromatography (SiO₂/petrol ether : ethyl acetate [5 : 1]) to give **20** (110 mg, 85%) as a dark red solid. M.p.: 183–184 °C; ¹H NMR (400 MHz, CDCl₃): δ = 8.67 (d, *J* = 8.1 Hz, 2H, *Pery-1H,6H*), 8.52–8.46 (m, 4H, *Pery-2H,5H,7H,12H*), 7.98 (d, *J* = 8.4 Hz, 1H, *Pery-8H*), 7.79 (approx. d, *J* = 8.6 Hz, 4H, (*t*-Bu)OOC-*Ph-2H,6H*), 7.69 (d, *J* = 7.8 Hz, 1H, *Pery-10H*), 7.64 (t, *J* = 7.9 Hz, 1H, *Pery-11H*), 7.49 (t, *J* = 7.7 Hz, 1H, *Ph-4H*), 7.44 (d, *J* = 8.6 Hz, 2H,

TPA-Ph-3H,5H), 7.35 (d, $J = 7.8$ Hz, 2H, *Ph-3H,5H*), 7.15 (m, 2H, *Th-3H, Th'-4H*), 7.12–7.06 (m, 6H, (*t*-Bu)OOC-*Ph-3H,5H, TPA-Ph-2H,6H*), 2.75–2.65 (m, 4H, *Th- α -CH₂, Ph-CH-(CH₃)₂*), 2.44 (t, $J = 7.6$ Hz, 2H, *Th- α -CH₂*), 1.70 (quin, $J = 6.8$ Hz, 2H, *Th- β' -CH₂*), 1.59 (s, 18H, C-(*CH₃*)₃), 1.55 (quin, $J = 6.8$ Hz, 2H, *Th- β -CH₂*), 1.45–1.40 (m, 2H, *Th- γ' -CH₂*), 1.39–1.30 (m, 4H, *Th-CH₂*), 1.20–1.10 (m, 6H, *Th-CH₂*), 1.19 (d, $J = 6.8$ Hz, 12H, *Ph-CH-(CH₃)₂*), 0.89 (t, $J = 6.8$ Hz, 3H, *Th'-CH₃*), 0.77 (t, $J = 6.9$ Hz, 3H, *Th-CH₃*); ¹³C NMR (100 MHz, CDCl₃): $\delta = 165.27, 163.97, 150.23, 146.42, 145.70, 142.05, 139.53, 137.53, 137.25, 135.34, 134.97, 134.71, 134.49, 133.86, 132.69, 132.43, 132.11, 132.07, 131.01, 130.51, 130.39, 129.47, 128.26, 127.66, 127.37, 126.91, 126.83, 124.89, 124.03, 123.20, 123.12, 121.15, 120.89, 120.39, 118.53, 93.72, 82.99, 80.78, 31.68, 31.47, 30.48, 30.45, 29.38, 29.20, 29.15, 28.99, 28.90, 28.23, 24.03, 22.63, 22.49, 14.12, 14.02$; HRMS (MALDI-TOF) m/z : [M]⁺ calcd for C₈₄H₈₄N₂O₆S₂, 1280.577; found, [M + H]⁺ 1281.578.

4,4'-(4-({5'-([N-(2,6-Diisopropylphenyl)]-9-perylenyl-3,4-dicarboximide)-3',4-dihexyl-2,2'-bithien-5-yl}ethynyl)phenyl)imino]dibenzoate (2). Triad **20** (37 mg, 29 μ mol) was dissolved in 1 mL THF. To the resulting solution 1 mL of a 1 M methanolic lithium hydroxide solution (27 eq.) was added and the resulting solution was stirred for 4 h at 70 °C. After the reaction was completed the mixture was poured into water and was acidified with 1 M HCl (pH = 1). The organic layer was separated while the aqueous phase was extracted with dichloromethane. The combined organic phases were dried over magnesium sulfate and the solvent was removed by rotary evaporation. The crude product was purified by column chromatography (SiO₂/dichloromethane : acetic acid [50 : 1]) and was dried in vacuum to give **2** (20 mg, 60%) as a dark red solid. M.p.: 227–228 °C; ¹H NMR (400 MHz, CDCl₃): $\delta = 8.67$ (d, $J = 7.8$ Hz, 2H, *Pery-1H,6H*), 8.50–8.40 (m, 4H, *Pery-2H,5H,7H,12H*), 8.03 (d, $J = 8.6$ Hz, 4H, *HOOC-Ph-2H,6H*), 7.98 (d, $J = 8.3$ Hz, 1H, *Pery-8H*), 7.68 (d, $J = 7.8$ Hz, 1H, *Pery-10H*), 7.64 (t, $J = 7.9$ Hz, 1H, *Pery-11H*), 7.51–7.45 (m, 3H, *Ph-4H, TPA-Ph-3H,5H*), 7.35 (d, $J = 7.6$ Hz, 2H, *Ph-3H,5H*), 7.19–7.12 (m, 8H, *Th-3H, Th'-4H, HOOC-Ph-3H,5H, TPA-Ph-2H,6H*), 2.85–2.75 (m, 4H, *Th- α -CH₂, Ph-CH-(CH₃)₂*), 2.45 (t, $J = 7.3$ Hz, 2H, *Th- α -CH₂*), 1.70 (quin, $J = 7.5$ Hz, 2H, *Th- β' -CH₂*), 1.55 (quin, $J = 7.1$ Hz, 2H, *Th- β -CH₂*), 1.45–1.37 (m, 2H, *Th- γ' -CH₂*), 1.37–1.30 (m, 4H, *Th-CH₂*), 1.20–1.10 (m, 6H, *Th-CH₂*), 1.19 (d, $J = 6.8$ Hz, 12H, *Ph-CH-(CH₃)₂*), 0.89 (t, $J = 6.8$ Hz, 3H, *Th'-CH₃*), 0.77 (t, $J = 6.9$ Hz, 3H, *Th-CH₃*); ¹³C NMR (100 MHz, CDCl₃): $\delta = 172.30, 164.93, 152.12, 146.80, 146.63, 142.99, 140.47, 138.45, 138.16, 136.22, 136.04, 135.61, 135.47, 134.75, 133.82, 133.52, 133.02, 132.80, 131.90, 131.42, 131.31, 130.38, 130.33, 129.16, 128.62, 128.27, 127.79, 126.65, 124.96, 124.87, 123.98, 122.03, 121.95, 121.66, 121.38, 121.30, 120.49, 94.43, 84.33, 32.59, 32.40, 31.40, 31.37, 30.30, 30.13, 30.08, 29.91, 29.82, 24.96, 23.55, 23.41, 15.04, 14.93$; MS (MALDI-TOF) m/z : [M]⁺ calcd for C₇₆H₆₈N₂O₆S₂, 1168; found [M + H]⁺, 1169. Elemental analysis: calcd (%) for C₇₆H₆₆N₂O₆S₂: C 78.05, H 5.86, N 2.40; found C 78.21, H 5.99, N 2.33%.

4,4'-(4-({5'-([N-(2,6-Diisopropylphenyl)]-9-perylenyl-3,4-dicarboximide)-3',4-dihexyl-2,2'-bithien-5-yl}ethynyl)phenyl)imino]dibenzoate (4). Triad **19** (37 mg, 29 μ mol) was dissolved in 1 mL THF. To the resulting solution 1 mL of a 1 M methanolic lithium

hydroxide solution (27 eq.) was added and the resulting solution was stirred for 8 h at 70 °C. After the reaction was completed the mixture was poured into water (5 mL) and was acidified with 1 M HCl (pH = 1). The organic layer was separated while the aqueous phase was extracted with dichloromethane. The combined organic phases were dried over sodium sulfate and the solvent was removed by rotary evaporation. The crude product was purified by column chromatography (SiO₂/dichloromethane : acetic acid [50 : 1]) and was dried in vacuum to give **4** (20 mg, 60%) as a dark red solid. M.p.: 218–219 °C; ¹H NMR (400 MHz, THF-d₈): $\delta = 8.72$ –8.66 (m, 4H, *Pery-1H,6H, 2H,5H*), 8.62–8.59 (m, 2H, *Pery-7H, 12H*), 8.47 (d, $J = 8.5$ Hz, 1H, *Pery-8H*) 7.94 (d, $J = 8.7$ Hz, 4H (*t*-Bu)OOC-*Ph-2H,6H*), 7.79 (d, $J = 7.8$ Hz, 1H, *Pery-10H*), 7.72 (t, $J = 8.0$ Hz, 1H, *Ph-4H*), 7.49 (d, $J = 8.6$ Hz, 2H, *Ph-3H,5H*), 7.41–7.37 (m, *Pery-11H*) 7.32–7.28 (m, 3H, *Ph-3H,5H, Th'-4H*), 7.17–7.13 (m, 7H, *Th-3H, (t*-Bu)OOC-*Ph-3H,5H, TPA-Ph-2H,6H*), 2.93 (t, $J = 7.8$ Hz, 2H, *Th'- α -CH₂*), 2.84–2.76 (m, 4H, *Ph-CH-(CH₃)₂, Th- α -CH₂*), 1.83–1.73 (m, 4H, *Th- β' -CH₂, Th- β' -CH₂*), 1.53–1.31 (m, 12H, *-CH₂*), 1.14 (d, $J = 6.8$ Hz, 12H, *Ph-CH-(CH₃)₂*), 0.92 (t, $J = 7.3$ Hz, 3H, *Th'-CH₃*), 0.91 (t, $J = 7.4$ Hz, 3H, *Th-CH₃*); ¹³C NMR (100 MHz, THF-d₈): $\delta = 166.068, 163.323, 150.426, 148.187, 146.723, 145.847, 140.732, 139.234, 137.315, 136.981, 135.676, 134.773, 132.470, 132.390, 131.776, 131.705, 131.651, 131.475, 131.465, 131.080, 130.407, 129.605, 129.213, 128.908, 128.646, 128.544, 127.441, 127.080, 126.836, 125.896, 125.083, 124.446, 123.682, 123.328, 123.113, 121.392, 120.810, 120.697, 118.743, 118.480, 96.402, 81.792, 31.689, 31.670, 30.593, 30.194, 29.443, 29.278, 29.008, 28.942, 23.308, 22.585, 22.552, 13.474$; HRMS (MALDI-TOF) m/z : [M]⁺ calcd for C₇₆H₆₈N₂O₆S₂, 1168.452; found, [M + H]⁺ 1169.456.

***N,N*-Di(4-benzoic acid *tert*-butyl ester)-4-(4,3'-dihexyl-2,2'-bithien-5-yl)-phenylamine (22).** Bromobithiophene **12** (138 mg, 0.33 mmol) and triphenylamine boronic ester **21** (200 mg, 0.35 mmol) were dissolved in 5 mL THF. The resulting solution was carefully degassed and the catalyst (Pd(OAc)₂ (2.5 mol%), PPh₃) (10 mol%) and the base (2 M aqueous potassium phosphate solution (0.5 mL, 3 eq.)) were added. Next, the reaction mixture was carefully degassed and stirred at 80 °C overnight. After the reaction was completed the mixture was poured into saturated ammonium chloride solution (15 mL) and the organic layer was separated while the aqueous phase was extracted with diethylether. The combined organic phases were washed with brine, dried over sodium sulfate and the solvent was removed by rotary evaporation. The crude product was purified by column chromatography (SiO₂/*n*-hexane : ethyl acetate [92 : 8]) to give **22** (226 mg, 87%) as a bright yellow oil. ¹H NMR (400 MHz, CDCl₃): $\delta = 7.90$ (d, $J = 8.7$ Hz, 4H, (*t*-Bu)OOC-*Ph-2H,6H*), 7.39 (d, $J = 8.5$ Hz, 2H, *Ph-3H,5H*), 7.16–7.11 (m, 7H, (*t*-Bu)OOC-*Ph-3H,5H, Ph-2H,6H, Th'-5-H*), 6.99 (s, *Th-3-H*), 6.93 (d, $J = 5.1$ Hz, *Th'-4-H*), 2.79 (t, $J = 7.8$ Hz, 2H, *Th'- α -CH₂*), 2.67 (t, $J = 7.8$ Hz, 2H, *Th- α -CH₂*), 1.69–1.62 (m, 4H, β, β' -*CH₂*) 1.59 (s, 18H, *t*Bu-*CH₃*), 1.41–1.26 (m, 12H, *-CH₂*), 0.88 (t, $J = 6.8$ Hz, 6H, *Th-CH₃, Th'-CH₃*); ¹³C NMR (100 MHz, CDCl₃): $\delta = 165.38, 150.56, 145.37, 139.44, 139.02, 136.87, 134.29, 130.89, 130.76, 130.28, 130.08, 128.46, 126.37, 125.69, 123.46, 122.780, 80.81, 31.72, 31.68, 30.93, 30.72, 29.30, 29.27, 29.20, 28.85, 28.26, 22.66, 22.63, 14.14$; HRMS (MALDI-TOF) m/z : [M]⁺ calcd for C₄₈H₅₉NO₄S₂, 777.389; found, [M]⁺ 777.388.

***N,N*-Di(4-benzoic acid *tert*-butyl ester)-4-(5'-(5-bromo-4,3'-dihexyl-2,2'-bithien-5-yl)-phenylamine) (23).** Bithiophene-triphenylamine **22** (92.9 mg, 0.12 mmol) was dissolved in 2 mL dry DMF and stirred at $-20\text{ }^{\circ}\text{C}$ under light protection. *N*-Bromosuccinimide (21.2 mg, 0.12 mmol) dissolved in 1 mL dry DMF was added dropwise in 1 h. Next, the reaction mixture was stirred overnight at room temperature. After the reaction was completed the mixture was poured into half saturated ammonium chloride solution (10 mL) and the organic phase was extracted with diethylether. The combined organic phases were washed with brine, dried over sodium sulfate and the solvent was removed by rotary evaporation. The crude product was purified by column chromatography (SiO_2/n -hexane : ethyl acetate [95 : 5]) to give **23** (86 mg, 80%) as a viscous yellow oil. ^1H NMR (400 MHz, CDCl_3): $\delta = 7.82$ (d, $J = 8.8$ Hz, 4H, (*t*-Bu)OOC-*Ph*-2*H*,6*H*), 7.37 (d, $J = 8.6$ Hz, 2H, *Ph*-3*H*,5*H*), 7.15–7.11 (m, 6H, (*t*-Bu)OOC-*Ph*-3*H*,5*H*, *Ph*-2*H*,6*H*), 6.92 (s, *Th*-3-*H*), 6.89 (s, *Th'*-4-*H*), 2.72 (t, $J = 7.8$ Hz, 2H, *Th'*- α - CH_2), 2.67 (t, $J = 7.8$ Hz, 2H, *Th*- α - CH_2), 1.69–1.62 (m, 4H, β , β' - CH_2) 1.51 (s, 18H, *t*Bu- CH_3), 1.38–1.26 (m, 12H, - CH_2 -), 0.88 (t, $J = 6.8$ Hz, 6H, *Th*- CH_3 , *Th'*- CH_3); ^{13}C NMR (100 MHz, CDCl_3): $\delta = 165.31, 150.47, 145.49, 139.96, 139.05, 137.40, 132.86, 132.63, 132.25, 130.85, 130.52, 130.23, 128.77, 126.39, 125.58, 122.79, 122.75, 110.05, 80.78, 31.60, 30.84, 30.53, 29.17, 29.11, 29.09, 28.74, 28.21, 22.57, 14.07$; MS (MALDI-TOF) m/z : [M] $^+$ calcd for $\text{C}_{48}\text{H}_{58}\text{BrNO}_4\text{S}_2$, 855; found [$\text{M} + \text{H}$] $^+$, 856.

***N,N*-Di(4-benzoic acid *tert*-butyl ester)-4-(5'-(4,4,5,5-tetramethyl-1,3,2-dioxaborolane-2-yl)-4,3'-dihexyl-2,2'-bithien-5-yl)-phenylamine (24).** Isopropylmagnesium chloride (0.32 mL, 0.64 mmol, 2 M in THF) was added dropwise to a suspension of lithium chloride (20 mg, 0.48 mmol) in 1 mL dry THF and stirred until lithium chloride was completely dissolved. 0.33 mL of the resulting solution was then added to a solution of brominated bithiophene-triphenylamine **23** (51 mg, 0.06 mmol) in 1 mL dry THF at $0\text{ }^{\circ}\text{C}$. Next, the resulting reaction mixture was stirred for 1 h until it was warmed up to room temperature. Then 2-isopropoxy-4,4,5,5-tetramethyl-1,3,2-dioxaborolane was added at once and the reaction mixture was stirred overnight. After the reaction was completed the mixture was poured into saturated ammonium chloride solution (10 mL) and the organic phase was extracted with diethylether. The combined organic phases were washed with brine, dried over sodium sulfate and the solvent was removed by rotary evaporation. Boronic ester **24** was obtained as a yellow resin (54 mg, 50%) with a purity of 50% (^1H NMR). It was used without further purification. ^1H NMR (400 MHz, CDCl_3): $\delta = 7.89$ (d, $J = 8.8$ Hz, 4H, (*t*-Bu)OOC-*Ph*-2*H*,6*H*), 7.46 (s, 1H, *Th'*-4-*H*), 7.39 (d, $J = 8.5$ Hz, 2H, *Ph*-3*H*,5*H*), 7.15–7.12 (m, 6H, (*t*-Bu)OOC-*Ph*-3*H*,5*H*, *Ph*-2*H*,6*H*), 7.05 (s, *Th*-3-*H*), 2.79 (t, $J = 7.8$ Hz, 2H, *Th'*- α - CH_2), 2.67 (t, $J = 7.8$ Hz, 2H, *Th*- α - CH_2), 1.69–1.62 (m, 4H, β , β' - CH_2) 1.51 (s, 18H, *t*Bu- CH_3), 1.35–1.28 (m, 12H, - CH_2 -), 1.27 (s, 12H, B-C- CH_3), 0.88 (t, $J = 6.8$ Hz, 6H, *Th*- CH_3 , *Th'*- CH_3); MS (MALDI-TOF) m/z : [M] $^+$ calcd for $\text{C}_{54}\text{H}_{70}\text{BNO}_6\text{S}_2$, 903; found [$\text{M} + \text{H}$] $^+$, 904.

***N,N*-Di(4-benzoic acid *tert*-butyl ester)-4-(5'-(*N*-(2,6-diisopropylphenyl)-perylene-3,4-dicarboximide-9-yl)-4,3'-dihexyl-2,2'-bithien-5-yl)-phenylamine (25).** Bromoperylene **15** (15 mg, 28 μmol) and bithiophene triphenylamine boronic ester **24**

(26 mg, 29 μmol) were dissolved in 3 mL THF. The resulting solution was carefully degassed and the catalyst ($\text{Pd}(\text{PPh}_3)_4$ (10 mol%)) and the base (2 M aqueous potassium phosphate solution (0.04 mL, 3 eq.)) were added. Next, the reaction mixture was carefully degassed and stirred at $80\text{ }^{\circ}\text{C}$ for 2 h. After the reaction was completed the mixture was poured into water (10 mL) and the organic layer was separated while the aqueous phase was extracted with dichloromethane. The combined organic phases were dried over sodium sulfate and the solvent was removed by rotary evaporation. The crude product was purified by column chromatography (SiO_2/n -hexane : ethyl acetate [4 : 1]) to give **25** (30 mg, 88%) as a black solid. M.p.: $179\text{--}180\text{ }^{\circ}\text{C}$; ^1H NMR (400 MHz, CDCl_3): $\delta = 8.67\text{--}8.64$ (m, 2H, *Pery*-1*H*,6*H*), 8.51–8.41 (m, 5H, *Pery*-2*H*,5*H*,7*H*,8*H*,12*H*), 7.92 (d, $J = 8.6$ Hz, 4H (*t*-Bu)OOC-*Ph*-2*H*,6*H*), 7.74 (d, $J = 7.9$ Hz, 1H, *Pery*-10*H*), 7.68 (t, $J = 7.9$ Hz, 1H, *Ph*-4*H*), 7.51–7.42 (m, 3H, *Pery*-11*H*, *Ph*-3*H*,5*H*), 7.35 (d, $J = 7.8$ Hz, 2H, *Ph*-3*H*,5*H*), 7.02–7.12 (m, 8H, *Th*-3*H*, *Th'*-4*H*, (*t*-Bu)OOC-*Ph*-3*H*,5*H*, *TPA*-*Ph*-2*H*,6*H*), 2.92 (t, $J = 7.8$ Hz, 2H, *Th'*- α - CH_2), 2.81–2.78 (m, 2H, *Ph*-CH-(CH_3) $_2$), 2.72 (t, $J = 7.8$ Hz, 2H, *Th*- α - CH_2), 1.82–1.65 (m, 4H, *Th*- β' - CH_2 , *Th*- β - CH_2), 1.60 (s, 18H, *t*Bu- CH_3), 1.39–1.29 (m, 12H, - CH_2 -), 1.20 (d, $J = 6.8$ Hz, 12H, *Ph*-CH-(CH_3) $_2$) 0.92 (t, $J = 6.7$ Hz, 3H, *Th'*- CH_3), 0.90 (t, $J = 6.6$ Hz, 3H, *Th*- CH_3); ^{13}C NMR (100 MHz, CDCl_3): $\delta = 165.32, 150.51, 146.54, 145.71, 145.56, 139.26, 132.01, 130.89, 130.27, 126.84, 126.49, 125.63, 123.99, 122.84, 120.94, 120.19, 80.79, 31.70, 31.64, 30.91, 30.70, 29.68, 29.31, 29.16, 28.24, 24.01, 22.65, 22.59, 14.09$; HRMS (MALDI-TOF) m/z : [M] $^+$ calcd for $\text{C}_{82}\text{H}_{84}\text{N}_2\text{O}_6\text{S}_2$, 1256.577; found, [$\text{M} + \text{H}$] $^+$ 1257.576.

***N,N*-Di(4-benzoic acid)-4-(5'-(*N*-(2,6-diisopropylphenyl)-perylene-3,4-dicarboximide-9-yl)-4,3'-dihexyl-2,2'-bithien-5-yl)-phenylamine (3).** Triad **25** (28 mg, 22 μmol) was dissolved in 0.5 mL dry dichloromethane. To the resulting solution 0.09 mL trifluoroacetic acid (1.1 mmol) was added and the deep violet solution was stirred for 6 h at room temperature. After the reaction was completed the solution was concentrated and the product was precipitated from *n*-hexane, filtered and dried in vacuum to give **3** (25 mg, 99%) as a black solid. M.p.: $210\text{--}212\text{ }^{\circ}\text{C}$; ^1H NMR (400 MHz, THF-d_8): $\delta = 8.68\text{--}8.65$ (m, 2H, *Pery*-1*H*,6*H*), 8.52–8.43 (m, 5H, *Pery*-2*H*,5*H*,7*H*,8*H*,12*H*), 8.04 (d, $J = 8.6$ Hz, 4H HOOC-*Ph*-2*H*,6*H*), 7.78 (d, $J = 7.8$ Hz, 1H, *Pery*-10*H*), 7.71 (t, $J = 7.9$ Hz, 1H, *Ph*-4*H*), 7.50–7.47 (m, 3H, *Pery*-11*H*, *Ph*-3*H*,5*H*), 7.35 (d, $J = 7.8$ Hz, 2H, *Ph*-3*H*,5*H*), 7.26–7.21 (m, 7H, *Th*-3*H*, HOOC-*Ph*-3*H*,5*H*, *TPA*-*Ph*-2*H*,6*H*), 7.13 (s, 1H, *Th'*-4*H*), 2.92 (t, $J = 7.8$ Hz, 2H, *Th'*- α - CH_2), 2.81–2.71 (m, 4H, *Ph*-CH-(CH_3) $_2$, *Th*- α - CH_2), 1.82–1.67 (m, 4H, *Th*- β - CH_2 , *Th*- β' - CH_2), 1.41–1.29 (m, 12H, - CH_2 -), 1.19 (d, $J = 6.8$ Hz, 12H, *Ph*-CH-(CH_3) $_2$) 0.93–0.88 (m, 6H, *Th*- CH_3 , *Th'*- CH_3); ^{13}C NMR (100 MHz, THF-d_8): $\delta = 166.92, 164.10, 151.43, 146.66, 146.59, 140.80, 139.95, 139.39, 138.33, 138.08, 137.74, 135.76, 134.32, 133.12, 133.07, 132.47, 132.31, 132.26, 131.82, 131.31, 131.13, 130.94, 130.28, 129.76, 129.60, 129.47, 129.43, 129.36, 129.27, 128.11, 127.54, 126.45, 126.32, 125.19, 124.48, 124.11, 123.56, 122.07, 122.03, 121.52, 121.38, 32.49, 32.43, 32.33, 31.62, 31.46, 30.16, 30.07, 29.89, 29.78, 29.42, 24.10, 23.37, 23.32, 14.27$; HRMS (MALDI-TOF) m/z : [M] $^+$ calcd for $\text{C}_{74}\text{H}_{68}\text{N}_2\text{O}_6\text{S}_2$, 1144.452; found, [M] $^+$ 1145.454.

Acknowledgements

The authors would like to thank the German Federal Ministry of Education and Research (BMBF) for funding our research on organic solar cell materials in the frame of a joint project. This work was also supported by the German Science Foundation (DFG) in the frame of a Collaborative Research Center (SFB) 569. We would also like to thank the Victorian Consortium for Organic Solar Cells (VICOSC), the ARC Centre of Excellence for Electromaterials Science (ACES) and the German Academic Exchange Service (DAAD-Go8 joint research cooperation scheme) for financial support. Furthermore we would like to acknowledge the ARC for providing equipment support through LIEF, as well as supporting UB and AJM with an Australian Research Fellowship. Special thanks also to Monash University for supporting U.B. with a Monash Research Fellowship.

References

- B. O'Regan and M. Grätzel, *Nature*, 1991, **353**, 737.
- A. Hagfeldt and M. Grätzel, *Acc. Chem. Res.*, 2000, **33**, 269.
- M. Grätzel, *Acc. Chem. Res.*, 2009, **42**, 1788.
- C.-Y. Chen, M. Wang, J.-Y. Li, N. Pootrakulchote, L. Alibabaei, C.-H. Ngoc-le, J.-D. Decoppet, J.-H. Tsai, C. Grätzel, C.-G. Wu, S. M. Zakeeruddin and M. Grätzel, *ACS Nano*, 2009, **3**, 3103.
- Q. Yu, Y. Wang, Z. Yi, N. Zu, J. Zhang, M. Zhang and P. Wang, *ACS Nano*, 2010, **4**, 6032.
- A. Mishra, M. K. R. Fischer and P. Bäuerle, *Angew. Chem., Int. Ed.*, 2009, **48**, 2474.
- A. Hagfeldt, G. Boschloo, L. Sun, L. Kloo and H. Pettersson, *Chem. Rev.*, 2010, **110**, 6595.
- J. He, H. Lindström, A. Hagfeldt and S. E. Lindquist, *J. Phys. Chem. B*, 1999, **103**, 8940.
- A. Morandeira, G. Boschloo, A. Hagfeldt and L. Hammarström, *J. Phys. Chem. B*, 2005, **109**, 19403.
- A. Morandeira, G. Boschloo, A. Hagfeldt and L. Hammarström, *J. Phys. Chem. C*, 2008, **112**, 9530.
- Y. Mizoguchi and S. Fujihara, *Electrochem. Solid-State Lett.*, 2008, **11**, K78.
- A. Nattestad, M. Ferguson, R. Kerr, Y.-B. Cheng and U. Bach, *Nanotechnology*, 2008, **19**, 295304, (9pp).
- (a) A. Morandeira, J. Fortage, T. Edvinsson, L. Le Pleux, E. Blart, G. Boschloo, A. Hagfeldt, L. Hammarström and F. Odobel, *J. Phys. Chem. C*, 2008, **112**, 1721; (b) L. Le Pleux, A. L. Smeigh, E. Gibson, Y. Pellegrin, E. Blart, G. Boschloo, A. Hagfeldt, L. Hammarstrom and F. Odobel, *Energy Environ. Sci.*, 2011, **4**, 2075.
- P. Qin, H. Zhu, T. Edvinsson, G. Boschloo, A. Hagfeldt and L. Sun, *J. Am. Chem. Soc.*, 2008, **130**, 8570.
- P. Qin, M. Linder, T. Brinck, G. Boschloo, A. Hagfeldt and L. Sun, *Adv. Mater.*, 2009, **21**, 2993.
- S. Sumikura, S. Mori, S. Shimizu, H. Usami and E. Suzuki, *J. Photochem. Photobiol., A*, 2008, **194**, 143.
- A. Nattestad, X. Zhang, U. Bach and Y.-B. Cheng, *J. Photonics Energy*, 2011, **1**, 011103.
- A. Nattestad, A. J. Mozer, M. K. R. Fischer, Y. B. Cheng, A. Mishra, P. Bäuerle and U. Bach, *Nat. Mater.*, 2010, **9**, 31.
- A. Listorti, B. O'Regan and J. R. Durrant, *Chem. Mater.*, 2011, **23**, 3381.
- P. Qin, J. Wiberg, E. A. Gibson, M. Linder, L. Li, T. Brinck, A. Hagfeldt, B. Albinsson and L. Sun, *J. Phys. Chem. C*, 2010, **114**, 4738.
- S. Mori, S. Fukuda, S. Sumikura, Y. Takeda, Y. Tamaki, E. Suzuki and T. Abe, *J. Phys. Chem. C*, 2008, **112**, 16134.
- Z. Ji, G. Natu, Z. Huang and Y. Wu, *Energy Environ. Sci.*, 2011, **4**, 2818.
- Y.-S. Yen, W.-T. Chen, C.-Y. Hsu, H.-H. Chou, J. T. Lin and M.-C. P. Yeh, *Org. Lett.*, 2011, **13**, 4930.
- J. Lee, R. Velarde-Ortiz, A. Guijarro, J. R. Wurst and R. D. Rieke, *J. Org. Chem.*, 2000, **65**, 5428.
- R. M. Keefer and L. J. Andrews, *J. Am. Chem. Soc.*, 1956, **78**, 5623.
- J. Cremer, E. Mena-Osteritz, N. G. Pschierer, K. Müllen and P. Bäuerle, *Org. Biomol. Chem.*, 2005, **3**, 985.
- Q. Wang, S. M. Zakeeruddin, J. Cremer, P. Bäuerle, R. Humphry-Baker and M. Grätzel, *J. Am. Chem. Soc.*, 2005, **127**, 5706.
- J. Cremer, PhD thesis, University of Ulm, Ulm, 2005.
- Z.-S. Wang, Y. Cui, K. Hara, Y. Dan-oh, C. Kasada and A. Shinpo, *Adv. Mater.*, 2007, **19**, 1138.
- M. Xu, S. Wenger, H. Bala, D. Shi, R. Li, Y. Zhou, S. M. Zakeeruddin, M. Grätzel and P. Wang, *J. Phys. Chem. C*, 2009, **113**, 2966.
- A. Mishra, C.-Q. Ma, R. A. J. Janssen and P. Bäuerle, *Chem.-Eur. J.*, 2009, **15**, 13521.
- A. J. Mozer, D. K. Panda, S. Gambhir, B. Winther-Jensen and G. G. Wallace, *J. Am. Chem. Soc.*, 2010, **132**, 9543.